Research Square

Preprints are preliminary reports that have not undergone peer review.
They should not be considered conclusive, used to inform clinical practice,
or referenced by the media as validated information.

Multimodal Characterization of the Tin Relief Decorations on the Van Eyck's Ghent Altarpiece and Their Degradation Process

Sophie Kirkpatrick
Royal Institute of Cultural Heritage (KIK-IRPA)
Jana Sanyova
Royal Institute of Cultural Heritage (KIK-IRPA)
Koen Janssens
University of Antwerp (UA), ARCHES and AXIS research groups
Helene Dubois
Royal Institute of Cultural Heritage (KIK-IRPA)
Ingrid Geelen
Royal Institute of Cultural Heritage (KIK-IRPA)
Marcus Koch
HTW Saar - University of Applied Sciences
Christine Berberich
Technical University of Munich
Cecile Glaude
Royal Institute of Cultural Heritage (KIK-IRPA)
Martina Stillhammerova
Royal Institute of Cultural Heritage (KIK-IRPA)
Louise Decq
Royal Institute of Cultural Heritage (KIK-IRPA)
Ermanno Avranovich Clerici
University of Antwerp (UA), AXIS research group
Steven De Meyer
Royal Institute of Cultural Heritage (KIK-IRPA)
Andrea Marchetti
University of Antwerp (UA), ARCHES and AXIS research groups
Victoria Beltran
University of Antwerp (UA), AXIS research group
Ferenc Borondics
SMIS beamline
Annelies Rios-Casier

University of Antwerp (UA), ARCHES and AXIS research groups

Alina Krotova

University of Antwerp (UA), ARCHES and AXIS research groups

Geert Van der Snickt

geert.vandersnickt@uantwerpen.be

University of Antwerp (UA), ARCHES and AXIS research groups

Article

Keywords: Tin degradation, tin soaps, MA-XRPD, OPT-IR, brocades, Ghent Altarpiece, Van Eyck

Posted Date: June 22nd, 2026

DOI: https://doi.org/10.21203/rs.3.rs-9941906/v1

License: This work is licensed under a Creative Commons Attribution 4.0 International License.
Read Full License

Additional Declarations: No competing interests reported.

MULTIMODAL CHARACTERIZATION OF THE TIN RELIEF DECORATIONS ON THE VAN EYCK'S GHENT ALTARPIECE AND THEIR DEGRADATION PROCESS.

S. Kirkpatrick[1,2], J. Sanyova[1], K. Janssens[3], H. Dubois[1], I. Geelen[1], M. Koch[4], C. Berberich[5], C. Glaude[1], M. Stillhammerova[1], L. Decq[1], E. Avranovich Clerici[3], S. De Meyer[1,3], A. Marchetti[2,6], V. Beltran[3,7], F. Borondics[8], Annelies Rios-Casier[2], Alina Krotova[2] and G. Van der Snickt[2*].

[1] Royal Institute of Cultural Heritage (KIK-IRPA), Parc du Cinquantenaire 1, B-1000 Bruxelles, Belgium
[2] University of Antwerp (UA), ARCHES and AXIS research groups, Mutsaardstraat 31, B-2000 Antwerpen, Belgium
[3] University of Antwerp (UA), Department of Physics, AXIS research group, Groenenborgerlaan 171, B-2020 Antwerp, Belgium
[4] HTW Saar - University of Applied Sciences, Goebenstraße 40, 66117 Saarbrücken, Germany
[5] Technical University of Munich, Chair of Conservation-Restoration, Art Technology and Conservation Science, Oettingenstraße 15, 80538 Munich, Germany
[6] Royal Museums of Art and History (KMKG-MRAH), Parc du Cinquantenaire 10, B-1000 Bruxelles, Belgium
[7] Royal Museum for Central Africa (KMMA-MRAC), Leuvensesteenweg 13, 3080 Tervuren, Belgium
[8] SMIS beamline, Synchrotron Soleil, L'Orme des Merisiers, Saint-Aubin, BP48, 91192 Gif-sur-Yvette, France

* corresponding author: geert.vandersnickt@uantwerpen.be

The recent conservation and restoration phases of The Ghent Altarpiece have astonished scholars and the public alike by revealing the exceptional original brushwork of Jan and Hubert van Eyck. Yet some of the polyptych's most intricate and enigmatic features remain under investigation: the applied brocades that form the richly decorated cloths of honour behind the Deity, the Virgin, and John the Baptist. To imitate the lustre and texture of luxurious silk and gold-threaded fabrics, the Van Eycks employed a highly sophisticated gilded tin-relief technique. These brocades, now heavily overpainted due to early degradation, present substantial challenges for conservation while offering a rare opportunity to study one of the few surviving prime examples of this demanding method. An extensive multimodal analytical campaign was undertaken to (a) identify remaining original metal-relief areas within surfaces repeatedly impacted by past interventions, (b) characterise the materials and layer stratigraphy, (c) document the current state of conservation, and (d) elucidate ongoing degradation mechanisms. Non-invasive analyses on the panels included upright and stereo microscope-aided visual examination, Macroscopic X-ray Fluorescence (MA-XRF) imaging, and Macroscopic X-ray Powder Diffraction (MA-XRPD). Complementary microanalyses on sampled material involved Field Emission Gun Scanning Electron Microscopy with Energy-Dispersive X-ray Spectroscopy (FEG-SEM-EDS), Fourier Transform Infrared Spectroscopy (μ-FTIR), Micro-Raman Spectroscopy (μRS), Optical Photothermal Infrared Spectroscopy (O-PTIR), and Synchrotron Radiation-based micro X-ray Powder Diffraction (μ-SR-XRPD). This study has directly informed ongoing treatment decisions and significantly advanced insight into the Van Eycks' innovative metal-relief technique—one of the earliest and most refined examples in European painting.

Key words: Tin degradation, tin soaps, MA-XRPD, OPT-IR, brocades, Ghent Altarpiece, Van Eyck

INTRODUCTION

The highly monitored conservation and restoration treatment of the Ghent Altarpiece began in 2012. Given the size of this pivotal artwork, the restoration campaign was divided into three successive phases: the first dedicated to the altarpiece exterior, the second to the lower register of the interior, and finally a third phase devoted to the upper register of the Altarpiece interior. During this last phase, started in May 2023, conservators and researchers faced a new challenge: the conservation of vulnerable polychromed and gilded tin foil-based reliefs, applied in the areas indicated in yellow in Fig.1. This sophisticated type of decoration, commonly referred to as "applied brocades", aimed to imitate luxurious cloth of honour stretched behind the three, almost life-size, central figures of the Virgin, the Deity, and John the Baptist [1, 2]. The tin-relief decorations have degraded very early in the

history of the panels and they underwent several overpaint and restoration campaigns in the past [2-7]. Today, pronounced crack patterns, brittle paint layers and loss of cohesion and adherence are particularly significant in these areas, and more pronounced when compared to the rest of the painted panels. Thereby, the applied brocades, of which the original purpose was to imitate both the texture and lustre of luxurious textiles made of gold and silk threads, are nowadays more difficult to read. It became soon clear to the conservators that characterising the employed materials, as well as their conservation state is necessary to better understand the decay of tin-relief decorations and to optimize treatment and preservation.

The origins and the technique of manufacture of applied brocades have been discussed in only a few publications [1, 8-12]. The oldest known examples of applied brocades are dated from the 1415-1430 and are localised in the Low Countries, Germany (Cologne, Berlin, Hamburg), and England (Norwich) [10-12]. This decorative technique became very popular in artworks from the middle of the fifteenth century and spread throughout Europe, until it fell out of favour by the mid-sixteenth century [1, 10, 12]. Descriptions of several case studies can be found in literature, on panel paintings [13-16], but also on sculptures or wall paintings [1, 8, 17-25]. Applied brocades can be found in geographical areas such as the Low Countries [1, 10, 14], Northern Spain [12, 17, 18, 23], Transylvania [24], Cologne [1, 15], England [1, 10, 19, 20], or France [1, 8, 11, 25]. These studies show that the overall layered structure of the brocades is consistent with that described in historical textual sources, in particular in *Il libro dell'arte* [26] and in the *Liber illuministarum*, also referred to as the "Tegernsee Manuscript" [9, 27-28]. These two manuscripts are dated to the late Middle Ages and are nowadays considered to provide the most relevant recipes for tin-relief decorations [1, 8-10]. The scheme in Fig. 2 illustrates the typical stratigraphy of an applied brocade. Basically, the manufacture of applied brocades starts with a tin foil (layer 6 in Fig. 2) pressed into a mould, providing the three-dimensional shape and volume of the brocade. This mould, probably made of wood or metal, was previously incised with a decorative pattern [1, 10]. Then, a pasty material (called *the filler* or *the mass, layer 4 in Fig. 2*) is spread over the tin foil to fill in the hollows. The excess of fill material is removed with a knife until a smooth surface is obtained [1, 10, 12]. Once the filler is dry, it fixes the reliefs and allows maintaining its shape during the demoulding and further handling of the tin foil. The ensuing 'reinforced' tin foil is then attached to the surface to be decorated, after an adhesive (layer 7 in Fig. 2) was applied on the mass-side of the brocade. Finally, the brocade is generally gilded with a mordant (layer 7 and 8 in Fig. 2) and partially covered with a coloured glaze or a matte paint (layer 9 in Fig.2), either before or after the aforementioned application [1, 9, 10]. Gilded stripes are left uncovered in order to imitate the gold threads, as demonstrated in Fig. 2. The applied brocades of the Ghent altarpiece are particularly refined. They exhibit very thin and delicate striations and an intricate design. They consist of rectangular sections (17 x 14 cm^2 on the panel of the Virgin and Saint John, and 19 x 12 cm^2 on the panel of the Deity) attached side by side in order to produce a continuous and repetitive design.



Fig. 1: (a) *The Adoration of the Mystic Lamb (Ghent Altarpiece)*, by Hubert and Jan van Eyck (375 x 514 cm^2, completed by 1432). The RGB image shows the polyptych opened (interior), after the second phase of the restoration, i.e. with the lower register after treatment and the upper register still awaiting treatment. The location of the applied brocades is indicated by a yellow line in the three central panels of the upper register, depicting from left to right: the Virgin, the Deity, and John the Baptist. (Cathedral of Saint Bavo, Ghent; ©KIK-IRPA). Details of the brocades on the Virgin panel (b), Deity panel (c), and the Saint John panel (d).

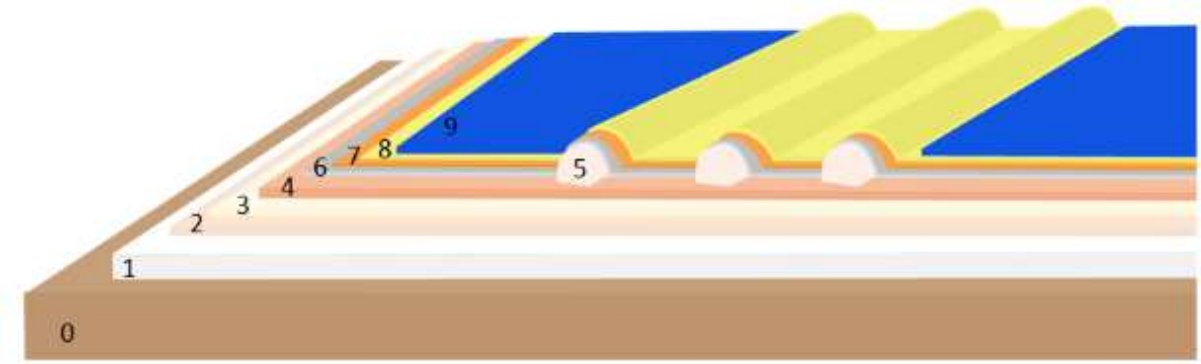


Fig. 2: Scheme showing the typical layer build-up of applied brocades, from bottom to top. Layer 0-3 is part of the traditional preparation of a panel painting: 0. Wooden support, 1. Ground, 2. Isolation, 3. Priming. Layer 4-9 is part of the build-up of a brocade: 4. Adhesive, 5. Filler (mass), 6. Tin foil, 7. Adhesive layer (mordant), 8. Gold leaf, and 9. Opaque paint and/or glaze.

The tin foil is an essential part of the applied brocades and plays a major role in the alteration of these areas. According to the existing literature, metallic tin is a relatively stable metal in clean, dry air at regular room temperatures; however, two main different types of degradation phenomena are known to affect this material: corrosion and so called 'tin pest' [21, 29-35]. The corrosion is a slow process that corresponds mainly to the oxidation of tin, giving rise to SnO (romarchite) and/or SnO_2 (cassiterite) [13, 21, 25, 36-41]. The corrosion of tin is strongly affected by the pH of its environment, and the contact with chemical pollutants, such as particular matter containing sulphates, nitrates and/or chlorides, that are usually found in normal atmospheric conditions [30, 32, 40]. Moreover, the oxidation rate of tin is influenced by the metallic impurities and alloy additions, in the sense that generally, it is known to increase with the presence of elements such as Mn, Sb, Bi, Pb, Fe and decreases with additions of Zn, In, Cd and P [21, 30, 37]. The second type of decay affecting tin is the named "tin pest". This phenomenon is due to a change in the crystalline structure, from the white beta metallic form (tetragonal) into the grey powdery non-metallic alpha form (cubic) [1, 21, 29, 30, 37, 39, 42]. This allotropic transformation takes place below 13.2°C. It is a slow process that is catalysed by humidity and influenced by the grain size (smaller grains are more prone to transformation), and by the presence of impurities and alloy additions [21, 30, 31-32]. Elements such as Sb, Bi, Pb, Ag, Cd can delay the transformation while Al, Zn, Ge, Cu accelerates it [30]. Both the corrosion and allotropic transformation of tin may cause similar deteriorations such as an increase in volume, cracks, loss of metallic appearance, the surface turning dark, grey, or white, exfoliations, decrease in cohesion, and loss of adherence of the tin foil with the support [21, 33, 39, 41, 42].

Today, medieval and later tin-foil based reliefs applied on artworks are usually found to be very degraded. On the Ghent altarpiece, the areas covered with applied brocades are extremely fragile and present particularly complex challenges for the restorers. A detailed chemical investigation was conducted to objectively characterize the state of conservation of these areas and to try to understand which degradation mechanisms are involved. This paper presents the insights gained from an analytical campaign conducted in two phases, as described by Van der Snickt et al. [43] Non-invasive analyses were first conducted in situ on the panels (MA-XRF, MA-XRPD), followed by chemical analyses applied on a selection of micro-samples (µ-FTIR, µRS, THM-GCMS, SEM-EDX, FEG-SEM, SR µ-XRPD). In addition to providing material information for the restorers and raising new research questions, it offers a privileged opportunity to study technical aspects of the manufacture of applied brocades by unravelling the material structure of these precious decorations.

MATERIALS AND METHODS

Macroscopic X-ray fluorescence (MA-XRF) imaging:

Each panel of the upper register of the altarpiece interior (Fig. 1) was entirely imaged by means of a MA-XRF scanner custom-built by the AXIS group of the University of Antwerp [44-46]. The X-ray source inside the measurement head is a 10W rhodium (energy 22.7 keV) anode transmission tube (Moxtex, UT, USA) and the secondary X-rays are detected by a Hitachi Vortex® EX-90 Silicon Drift Detector. The XRF measurement head is mounted on a software-controlled X–Y motor stage with a maximum travel range of 57 × 60 cm^2 (h × v) [44-46]. To cover the extension of each panel, measurements were divided into several overlapping scan areas and the MA-XRF scans were performed at a constant distance of ca. 2.5 cm between the measuring head and the painting. The data obtained were then processed by using PyMca (Python Multichannel Analyzer), Datamuncher and bAxil software packages, in order to visualise the spatial distribution of the characteristic X-ray emission lines of the different chemical elements on the painting. Grey scale maps for each element are obtained in which the grey level of each pixel corresponds to the intensity of the detected net XRF signal at the corresponding location. While reading the distribution maps, it must be considered that heavier elements absorb XRF radiation more readily than lighter elements [44, 46]. As a result, it is possible to see paint distributions containing heavier elements such as lead or mercury that were overpainted by paint containing lighter elements such as calcium or potassium, whereas the reverse is rarely possible.

Macroscopic X-ray powder diffraction (MA-XRPD):

Macroscopic X-ray powder diffraction measurements were performed by means of an in-house built mobile MA-XRPD scanner (AXIS, University of Antwerp, Belgium) [47-48]. The device is set-up with a low power X-ray micro source (50 W, IμS-Cu, Incoatec GmbH, Germany), which produces a monochromatic and focused X-ray beam (Cu–Kα; 8.04 keV) with a photon flux ≈ 2.9 × 10^8 photon/s ; (output focal distance: 20 cm, divergence: 2.4 mrad and a focal spot impinging on the sample with sizes around 140 μm in the vertical dimension and 800 μm in the horizontal one due to the Bragg-Brentano geometry employed for measurements) a PILATUS 200K (Dectris Ltd, Switzerland) area detector is used to record the 2D diffraction patterns. To reduce the effect of local topography and curvature of the painting surface on the diffraction data, the distance between the artwork and the scanner is automatically adjusted with a laser distance sensor (Baumer GmbH, Germany) at each measurement point. All components are placed on a motorized platform that is capable of moving in the X–Y–Z directions (30 x 30 x 10 cm^3). An area of 120 x 80 mm^2 on the artwork was scanned with a step size of 1.2 mm in both directions and an exposure time of 10 s per point. The diffraction data was processed using the in-house developed XRDUA software package and fitted using a whole pattern refinement procedure [47-48].

Cross sections:

In 1951, Paul Coremans, led a research and restoration campaign on the *Ghent Altarpiece* [2]. In this context, paint samples were taken and studied mainly as cross sections, sometimes as unmounted samples by means of microchemical (invasive) reactions [2, 5]. These samples were re-examined in the late 1980's [5] and in the current research campaign started in 2012 [4, 49]. In addition, new paint samples were taken where it was crucial to characterise and understand the layering structure and the materials composition. The recently taken samples from the applied brocades were embedded in a Technovit 2000 LC® resin. The resulting block was polished with a Labopol Struers® polisher until it reached the sample, then manually polished with micro mesh (granularity 3200–12.000). The manual polishing is the traditional method used for preparing the cross section. It is well adapted for the microscopical observation of paint layers and allows multiple analytical characterisations. However, it is less suitable for the sub-micro characterisation of metal foils, as this process inevitably leads to the

distortion of the metal layers within the stratigraphy. For this reason, a selection of cross sections was prepared with the Ion Milling System Hitachi IM 4000®, belonging to the Chair for Experimental Methodology of Material Science at Saarland University. Ion milling works on the principle of sputtering high energy ions (Ar^+) onto the surface to remove the top atomic layers of the sample and it allows to preserve the delicate structure of the stratigraphy [50, 51]. The analytical characterisation of the cross-sections was mainly performed at the Royal Institute for Cultural Heritage (KIKIRPA), where the samples are archived. Exceptionally, when a suitable method was not available in the KIKIRPA lab, the analyses were carried out in the laboratories of the project partners (LINM, ESRF, PETRA III (DESY), SMIS (SOLEIL)).

Optical microscopy (OM):

The cross sections were studied and photographed, with an upright optical microscope Axioplan (Carl Zeiss). Images were taken under white polarized light and UV illumination (excitation band-pass filter from 390-420 nm) with magnification up to 500x.

Scanning Electron Microscopy (SEM-EDX and FEG-ESEM-EDX):

The elemental composition of each layer of the embedded samples was determined, with a scanning electron microscopy with energy dispersive X-ray spectrometer (SEM-EDX) on a Zeiss - EVO LS15 microscope (15 kV) with BSE and EDX included (Oxford Instruments-X-MaxN 80mm, ASTEC-Oxford Instruments Software) at the KIKIRPA laboratory. In addition, a selection of samples was characterised at the INM-Leibniz Institute for New Materials with a high-resolution field emission gun environmental scanning electron microscope (FEG-ESEM-EDX) FEI Quanta 400 FEGat 10 kV accelerating voltage. This instrument is equipped with SE, backscatter, and EDS detectors, both high vacuum (ETD and SSD detectors) and low vacuum (LFD and SSD detectors) environments were used. The use of a FEG-ESEM is very suitable to observe the microstructure of samples as it can attain magnification levels between 50000x to 100000x.

Fourier Transform Infrared Spectroscopy by total attenuated reflectance (FTIR-ATR):

Analyses by total attenuated reflectance (FTIR-ATR) were performed on cross-sections using a Hyperion 3000 spectrometer coupled to a microscope with a tip of germanium (Ge) of 150 micrometres in diameter. FTIR-ATR signals between 4500 and 900 cm^{-1} were captured with a liquid nitrogen-cooled focal plane detector (FPA). The system allows the imaging of cross-sections and the collection of infrared spectra over large areas with a resolution of 4 cm^{-1}, using 128 scans.

Micro-Raman Spectroscopy (µRS)

The analyses were conducted with an instrument Renishaw InVia employing a red diode laser at 785 nm (Toptica photonique XTRA). The analyses are performed on cross-sections with a Leica DMLM microscope. The power of the laser can be varied between 0.1 and 5 mW; the magnification ranges from 20x to 100x, the number of accumulations varied from 1 to 10 times per measurement, and the scanning time selected from 10 to 80 s depending on the signal to noise ratio.

Thermally assisted Hydrolysis and Methylation Gas Chromatography/Mass Spectrometry (THM-GC/MS):

The samples that were not embedded were analysed by means of thermally assisted hydrolysis and methylation gas chromatography/mass spectrometry (THM-GC/MS). These analyses involve pyrolysing the sample into smaller components that are volatile enough for analysis. Since many of these smaller components contain polar groups that are difficult to separate on the chromatographic column, a simultaneous derivatization reaction is performed on the sample during the pyrolysis step

with tetramethylammonium hydroxide (TMAH), shielding polar groups through methylation. This makes certain fragments, such as fatty acids, more visible. The pyrolysis was carried out in the absence of oxygen, in a helium atmosphere at 480°C, in a Frontier Lab pyrolysis unit model 3030. The sample, supplemented with 4 µL TMAH (5% in methanol), is placed in a steel cup and dropped into a heated oven. The chromatographic column was connected directly to the pyrolysis unit, without using a conventional injector. A Supelco SLB-5ms column (20 m long, 0.18 mm internal diameter, 0.18 µm film thickness) was used for the chromatographic separation (Thermo TraceGC). The following temperature program was used: 1 min at 35°C, followed by heating at 10°C/min until reaching 240°C, then at 6°C/min to 315°C; finally, this temperature was maintained for 5 min. After separation, the components were detected with a mass spectrometer, which allows identification of the various separated components with high sensitivity (quadrupole MS, Thermo ISQ7000, scanned between 35 and 600 amu, MS at 240°C, transfer line at 270°C). The gas flow was programmed to increase with the rising of the oven temperatures. This results in better resolution at higher temperatures. The resulting pyrograms were scanned both manually and semi-automatically for marker components derived from natural or synthetic resins, waxes, oils, or proteins. Extensive reference databases were used for this. For the semi-automatic data processing, AMDIS (Automated Mass Spectral Deconvolution and Identification System) was used in combination with specific AMDIS target libraries, including the ESCAPE expert system.

Microscopic Synchrotron Radiation-based X-Ray Powder Diffraction (SR-based XRPD)

Submicroscopic SR-based XRPD measurements were performed at ID13 the microfocus beamline at the European Synchrotron Radiation facility (ESRF, Grenoble, France), within the frame of the «Historical Materials BAG»[52, 53]. ID13 is dedicated to high-lateral-resolution diffraction and scattering experiments using focused monochromatic X-ray beams. The measurements were performed on a selection of two samples from the Ghent Altarpiece (P.033.055 and P.033.057, localized in Fig. 5). Diffraction patterns were acquired in transmission geometry by means of an X-ray beam with a spot size of 2×2 µm^2, at an energy of 13 keV. XRPD maps are obtained by raster-scanning the samples and collecting 2D XRPD patterns, in transmission mode, with a Dectris EIGER 4 M single photon counting detector that acquires frames with 2070 × 2167 pixels (75 × 75 µm^2 pixel size) at a rate up to 750 Hz. A dwell time of 0.02 second per point was used during these scans thanks to the high photon flux (10^{14} photons/s) reached due to the recent Extremely Brilliant Source (EBS) upgrade.

Microscopic Synchrotron Radiation-based X-ray Fluorescence (SR-based XRF)

Fluorescence signals were collected from a selection of cross-sections (P259.25, P259.23, P033.29, P033.57, localised in Fig. 5) at the microprobe hutch of the Hard X-ray Micro/Nano-Probe Beamline P06 in Petra III, at DESY (Hamburg, Germany). This beamline is dedicated to scanning X-ray microscopy and diffraction with micro/nanoscopic spatial resolution [54]. A primary photon energy of 13.043 keV was employed for analyzing the paint cross-sections. This energy was chosen to be able to observe the Pb-L lines of lead and enhance its detection. XRF data were acquired with 0.2 seconds dwell times per scan pixel.

Optical Photothermal Infrared (O-PTIR) spectroscopy

O-PTIR measurements (spectra and images) were collected from a selection of two cross-sections (P.033.055 and P.033.058, localised in Fig. 5) on the mIRage Infrared Microscope (Photothermal Spectroscopy Corp.) at the SMIS beamline of Synchrotron Soleil. Spectra were collected in reflection mode, 2 cm^{-1} spectral data point spacing, through a 40x, 0.78 NA, 8 mm working distance Schwarzschild objective. The pump IR source was a pulsed, tunable four-stage QCL device, scanning from 928 to 1800 cm^{-1} and from 2800 to 3022 cm^{-1}. The pulse rate of this laser was 0.1 kHz, with a duty cycle of 1% and a pulse width of 100 ns. The probe was a CW 532 nm visible variable power laser

monitored by an APD detector. The power of both lasers has been optimized before the analysis in order to not cause damage to the sample. Specifically, the QCL laser power was set up at 10% while the probe laser power was set up at 1%. The spot size of the probe beam was 0.45 µm and the maps were collected using a step size of 1 µm in X and y axis. To obtain a good signal-to-noise ratio, 10 scans spectra were averaged at each point. O-PTIR data were treated using the Quasar 1.13.0 software [55, 56]. The spectra shown were normalized by the min-max method using the most intense band. To ensure an unbiased comparison, no smoothing, baseline correction or any other adjustment was applied to the spectra. Spectral maps were generated by plotting the integrated area of selected peaks with a linear baseline computed using two wavenumbers at the feet of the peak.

RESULTS

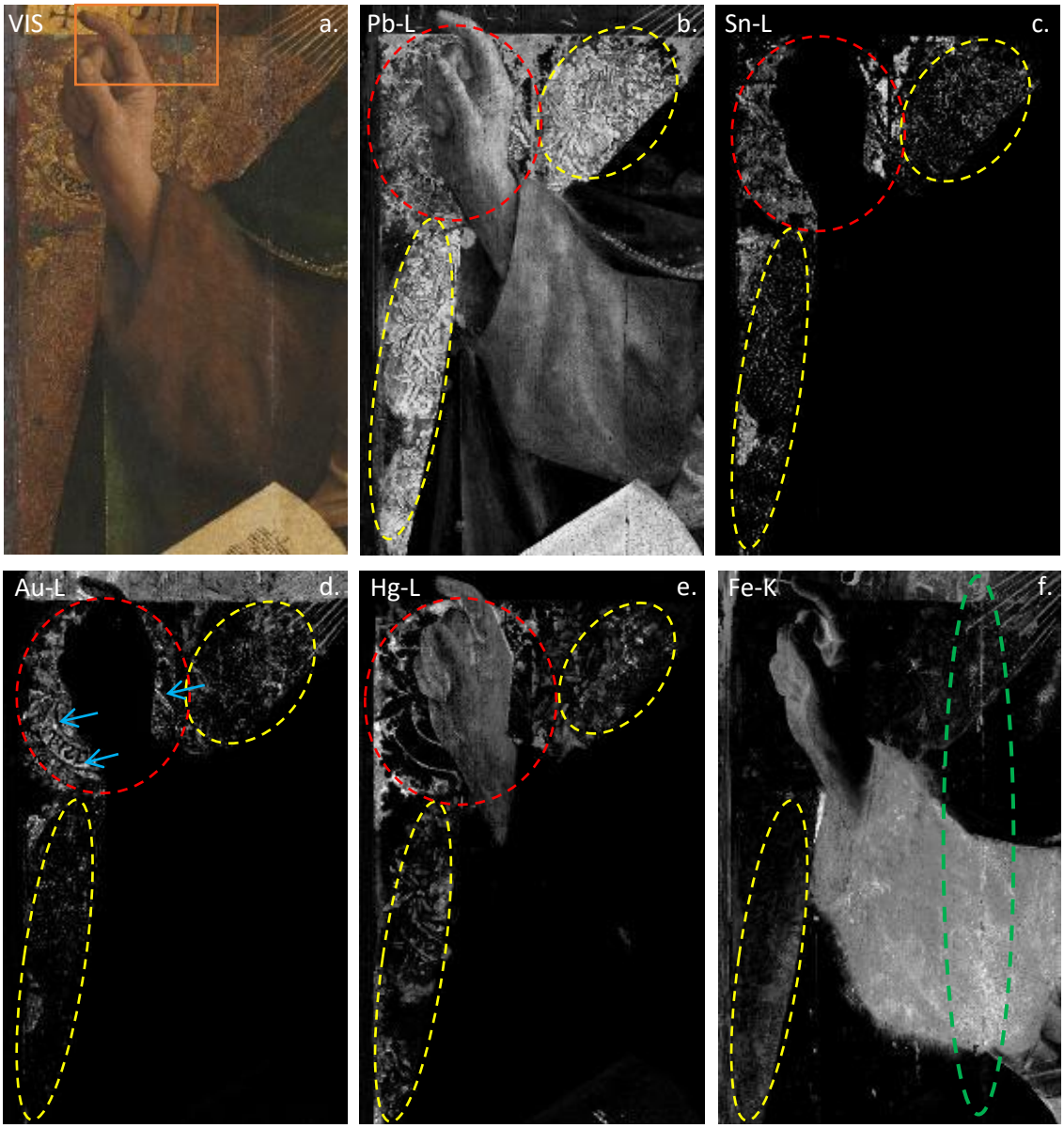
Differentiating original brocades from past interventions by non-invasive methods

MA-XRF imaging allowed for the precise documentation of past interventions on the panels such as: retouches and overpaints, in some cases covering paint losses. Therefore, this non-invasive method is essential to assess the general state of conservation of the panels. For instance, MA-XRF images show how three brocade motives along the clothes of Saint John (yellow dashed circles in Fig. 3b.) clearly exhibit more intense Pb-L signals than a third motive behind his hand (red dashed circle in Fig. 3b). The most intense lead signals are presumed to originate from the filler (layer 5 in Fig. 2), a lead-rich paste applied to the tin foil to support its relief, as explained in the introduction. The most intense lead signals have been associated with the filler, since the Pb-L distribution shows a pattern reminiscent of the knife resulting from the removal of excess material.

At the same time, the Sn-L and Au-L distribution maps (Fig. 3c. and d.) show that very little metallic tin and gold remained on these two motives. This confirms that the original metal foils largely disappeared in these areas, while revealing the filler underneath and accounting for the more intense lead signals at the same time. Interestingly, despite the loss of the gilded tin leaf in these areas, the three-dimensional volume and shape of the brocade motive is very well preserved. This shows that the filler plays an important role in the maintenance of the structure over time. In comparison, more tin and gold are detected in the motive closest to the hand (Fig. 3c and d, circled in red), which seems overall better preserved. In this area, the lead signal from the filler is attenuated and sheltered by the superimposed metal foils and thus less intense.

In addition, the MA-XRF experiments attest that the heavily applied brownish and pink retouching observed on the surface of the damaged areas contain barium, as indicated by the Ba-L distribution maps (Fig. 3i). In this context, intense barium signals are considered a marker of non-original interventions, as barium-based pigments were synthesised only from the late eighteenth century onwards [57-58], while minor barium signals can also occur due to a natural contamination of mineral pigments. Coinciding manganese and iron signals, indicative of the use of earth pigments such as Umber and Sienna, are also detected in the overpaints (yellow dashed circles in Fig. 3f. and 3g), as well as vermillion (HgS) (dashed yellow circles in Fig. 3c). An open joint between two boards of the wooden panel (Fig. 3f, g, and h. circled in green) was clearly filled and retouched with a calcium, manganese, and iron containing material. Finally, a careful inspection of the features of the gold distribution (Fig. 3d.) attests a separate intervention phase during which diagonal stripes with gold paint were applied locally to replace the original, gold leaf-based brocade. The gold paint is a gold powder dispersed in a viscous medium that was used to replicate the gilded relief of the brocade in several areas on the three panels to hide lacunae in the gold striations of the motives. In Fig. 3d (blue arrows) this gold inpainting can be recognized near the hand by the enhanced Au-L fluorescence signals.

Although the aforementioned local losses and repairs are perceptible by the trained eye of a conservator upon persistent visual examination (with or without the assistance of an optical stereomicroscope), MA-XRF images enable immediate, more complete and accurate classification and documentation of the original remains of metal sheets, while providing information on past treatment stages and the nature of the filler and intervention materials applied.



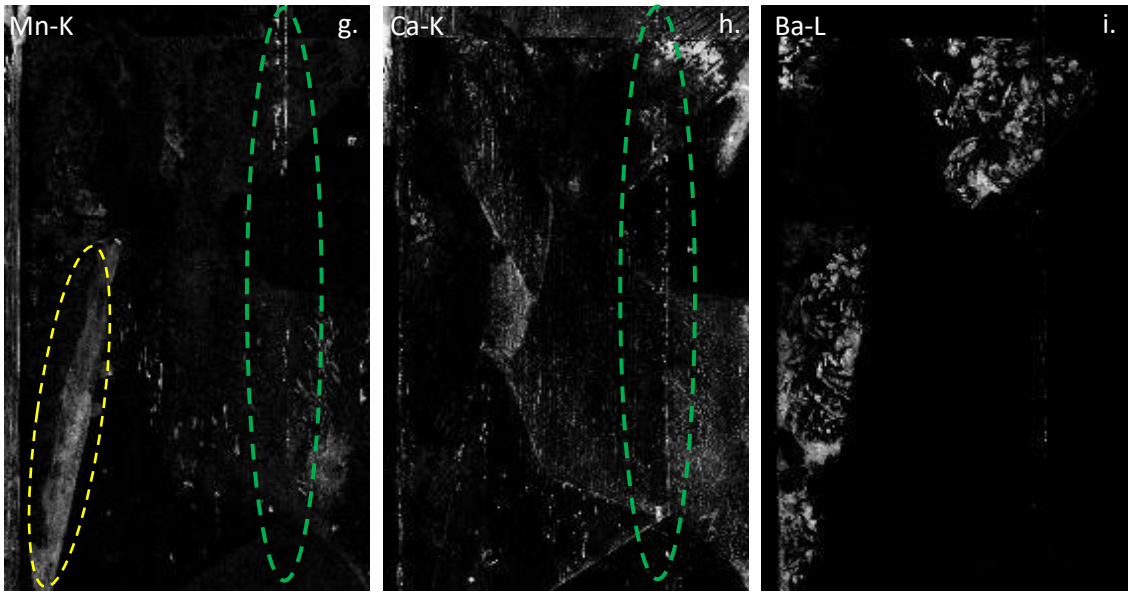


Fig. 3: (a) RGB image showing a detail of the panel of Saint John (©KIKIRPA). The orange square indicates the detail shown in Fig.4. (b-i) MA-XRF elemental images, showing the distribution of (b) lead (Pb–L), (c) tin (Sn–L), (d) gold (Au–L), (e) mercury (Hg–L), (f) iron (Fe–K), (g) manganese (Mn–K), (h) calcium (Ca–K), and (i) barium (Ba–L) and revealing a plenitude of material-technical information. The yellow dashed ellipses indicate largely disappeared brocade motives that were later retouched while the motive near the hand, indicated by the red dashed circle is better preserved. The green dashed ellipse signals a repaired and retouched panel joint.

As exemplified by the Saint John detail in Fig. 3, combining MA-XRF images with (stereomicroscopy-aided) visual examination has allowed to detect several types of past interventions on the applied brocades of the three central panels. Overall, it was highlighted that the condition of the applied brocades is very variable. They are well-preserved in several places (such as in the motives circled in red in Figs. 3b-e), while other areas show numerous losses. In the damaged areas, various fillings, local retouches, overpaints, and partial regilding are detected, attesting a multitude of past interventions (Figs. 3d-i)

However, while macro X-ray fluorescence (MA-XRF) scanning provides elemental distribution maps, it does not reveal the crystal structure or precise chemical environment of the detected elements. Consequently, a comprehensive identification of paint materials and especially their secondary degradation products remain unattainable based on MA-XRF data alone. In order to further enhance the understanding of the state of conservation of the fragile brocades, on-site macro X-ray powder diffraction (MA-XRPD) scanning was also conducted. Results of the combined MA-XRF/MA-XRPD measurements are exemplified in Fig. 4, that shows a detail of of the panel of Saint John. Meticulous examination of the elemental distribution of tin provides an assessment of the foil's overall condition, allowing differentiation between well-preserved regions and areas in which tin is absent. Nevertheless, interpretation of the tin mapping necessitates particular caution and must be undertaken in conjunction with direct visual inspection, as the presence of lead in certain overpaints can obscure the lower-energy tin signal underlying these layers. In a complementary manner, MA-XRPD allowed collecting additional information regarding the condition of the tin foil by revealing two types of tin oxides: romarchite (SnO) and cassiterite (SnO_2) as seen in Fig. 4. The distribution follows closely that of the Sn-K emission lines, indicating that the remaining tin is significantly oxidised. [9, 13, 33, 36]. Romarchite and cassiterite are two typical corrosion products generally encountered in degraded tin foils. SnO is typically black in appearance, whereas SnO_2 can exhibit a wide range of colors, including black, brownish black, reddish brown, red, yellow, grey, and white. Both compounds are opaque, brittle, and crystalline in nature.

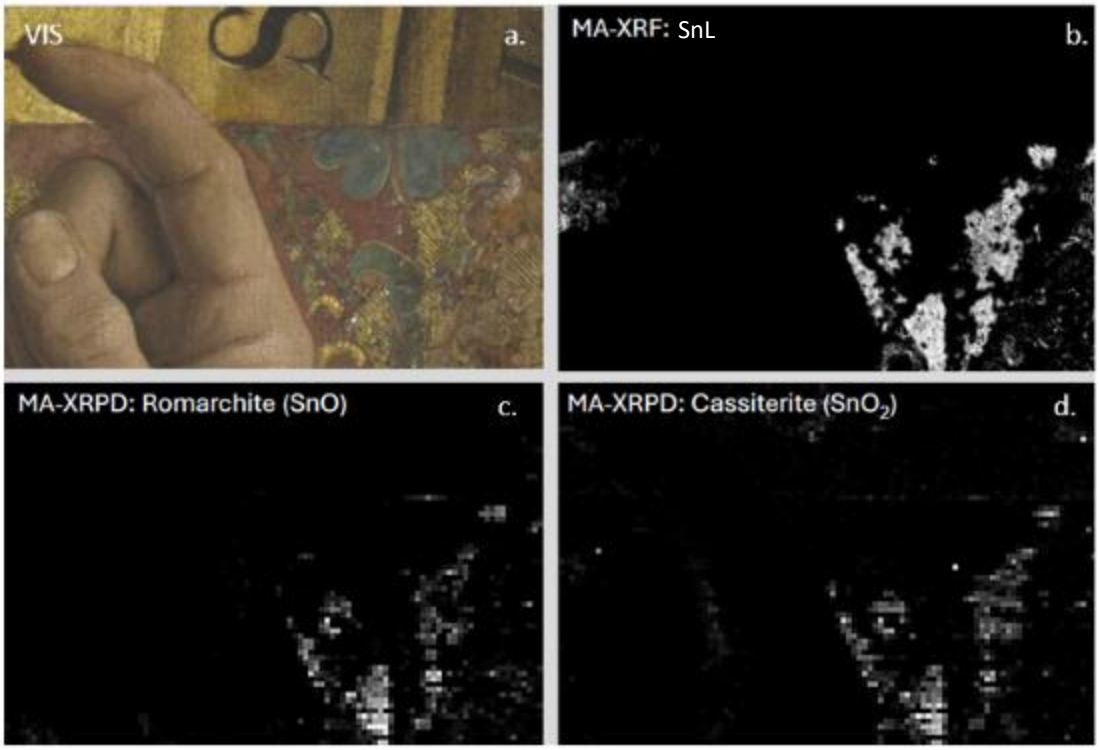


Fig. 4: (a) RGB image showing a detail of the panel of Saint John, indicated by the orange rectangle in Fig. 3a (©KIKIRPA). (b) MA-XRF elemental image showing the distribution of Sn-L emission lines. (c-d) MA-XRPD images mapping the matching distribution of (c) romarchite and (d) cassiterite.

Despite the significant information provided by means of MA-XRF and MA-XRPD, the results collected with these diagnostic instruments are limited by a few factors. First, the information is often inadequately layer-specific for a comprehensive understanding of the stratigraphy. The interpretation is hampered by the fact that the information depth usually varies within one distribution image, due to the lateral variation of high Z elements (e.g. Pb) in the top layers that locally shield the secondary signals of lower energy stemming from deeper inside the paint build-up [45]. Moreover, MA-XRF is insensitive towards organic compounds, while MA-XRPD is limited to crystalline compounds, present in relative high concentrations. To improve our understanding of how specific materials are distributed over the layers in the paint build-up, and the possible formation of degradation products, it is advisable to combine the aforementioned non-invasive methods with analytical techniques of enhanced chemical selectivity (such as µ-FTIR and µRS); an approach that usually requires sample extraction. Nevertheless, also for the latter, the anterior non-invasive characterisation of the panels is essential, as it allows distinguishing well-preserved areas that are suitable for sampling, such as the area circled in red in Fig 3b-e.

Characterization of the materials and layer buildup of the applied brocades using sample analysis

Twelve micro-samples (mostly dating back to a conservation campaign carried out in 1950-51, with addition of a few new samples) were extracted from various locations on the applied brocades of the three central panels, as indicated in Fig. 5. Although several small variations were observed, a multi-analytical characterisation of the ensuing cross-sections highlighted the similarity in materials and build-up between the panels of the enthroned Virgin, John the Baptist, and the Deity. A summary of the common features is given in Table 1 (see also analytical data in supplementary information); this indicates that the method for applying the brocades corresponds to the typical *modus operandi* of

that time, as discussed in the introduction and rendered in the scheme in Fig. 2. It should be noted that the accumulated overpaints and non-original varnishes were not considered in this table.

Table 1: The build-up and the material composition obtained by means of SEM-EDX, FTIR, µRS, THM-GCMS and SR-XRPD analysis. Each layer of the stratigraphy is labelled with the corresponding number as in the scheme in Fig. 2.

Layer		Analytical results	Methods
9.	Paint	Oil-based paint layers with pigments that vary depending on the colour of the area, such as lead white (mainly cerussite $PbCO_3$ and hydrocerussite $2PbCO_3{\cdot}Pb(OH)_2$), azurite ($2CuCO_3{\cdot}Cu(OH)_2$), red earth (hematite Fe_2O_3) and red lake	SEM-EDX, FTIR, µRS
8.	Gold leaf	Metallic gold containing 0.7 to 1.5 weight % of silver	SEM-EDX
7.	Mordant	Dark brown-red layer visible under upright OM but too thin for selective analysis.	OM
6.	Tin foil	Metallic tin. Presence of lead and chlorine. Romarchite and cassiterite.	SEM-EDX, SR-XRPD, SR-XRF
5.	Filler	Mainly heat-bodied siccative oil (likely linseed oil), with beeswax, small amount of colophony, traces of rapeseed oil. Lead white, minium (Pb_3O_4, heterogeneously dispersed). Presence of lead stearates ($C_{36}H_{70}PbO_4$).	THM-GCMS SEM-EDX, FTIR, µRS, SR-XRPD
4.	Adhesive	Mainly heat bodied linseed oil, some beeswax and colophony, and traces of rapeseed oil. Iron oxide (goethite and hematite), vermillion, lead white (hydrocerussite and cerussite), calcium carbonate ($CaCO_3$), minium, and few of carbon black, bone white, and orpiment (As_2S_3 in such small amount it might be impurities). Presence of lead stearates.	THM-GCMS SEM-EDX, FTIR, µRS, SR-XRPD
3.	Priming	Oil-based layer * Lead white, calcium carbonate, with iron oxides (mainly goethite-rich ochre α-FeOOH), and few grains of carbon black	SEM-EDX, FTIR
2.	Isolation	Oil-based layer * Almost unpigmented, calcium carbonate detected in few cases, likely originating from the ground	THM-GCMS SEM-EDX, FTIR
1.	Ground layer	Animal glue * Calcium carbonate	THM-GCMS SEM-EDX, FTIR

*Results obtained during the previous conservation phases [49].

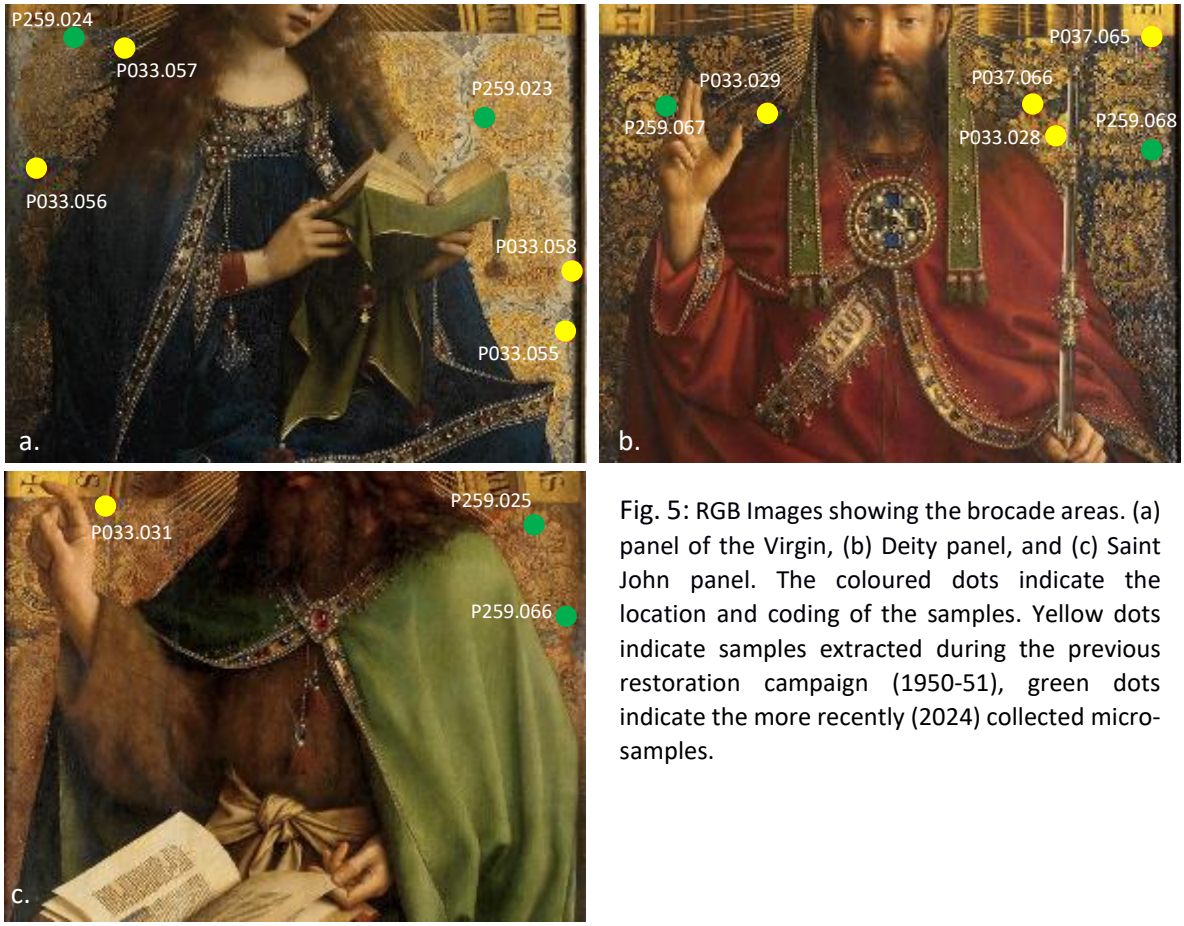


Fig. 5: RGB Images showing the brocade areas. (a) panel of the Virgin, (b) Deity panel, and (c) Saint John panel. The coloured dots indicate the location and coding of the samples. Yellow dots indicate samples extracted during the previous restoration campaign (1950-51), green dots indicate the more recently (2024) collected micro-samples.

When focusing on the strata that directly relate to the brocade (i.e. layers 4-8 in table 1 and Fig. 2), upright OM showed that the adhesive (layer 4) covering the priming is red/orange, as can be seen in Fig. 6. Upon studying the sampling site on the panel using a stereomicroscope, it becomes clear that the adhesive was applied with a brush, as areas lacking the upper layers (layers 5-9) reveal an orange adhesive layer with a distinct brush mark texture. THM-GC/MS analyses conducted on a selection of samples (P.259.024, P.259.068, P.259.025) from the panel of Virgin, the Deity, Saint John (see Fig. 5), suggested the presence of a siccative oil, likely linseed oil, as main component of the adhesive binder. The analyses also indicated few amounts of beeswax, and a pine resin, identified in particular. In addition to these substances, a protein fraction is also present in the adhesive. Proteins are poorly detected by THM-GC/MS due to their high fragmentation. Nevertheless, the presence of proteins in the samples is undeniable. The markers seem to indicate the presence of proteins associable to egg binder/varnish, although this cannot be confirmed with certainty by this technique. The adhesive is binder-rich and also contains a small amount of different pigments such as vermillion and lead white, whereas few particles of minium, calcium carbonate and iron oxide were identified with SEM-EDX, FTIR and µRS. Few grains of carbon black, bone white, and arsenic sulphide were detected as well, but in such small amount that these might be impurities. Finally, SR-XRPD analyses allowed to detect hydrocerussite, cerussite, and lead stearates.

The filler (layer 5), directly below the tin foil, is heterogeneously coloured, whitish in some areas and reddish in some others, as exemplified by the micrograph in Fig. 6 (the filler is highlighted by the red lines). THM-GC/MS analsyses of the aforementioned samples revealed a binder containing similar components to those identified in the adhesive, with a high concentration of siccative oil, along with small amounts of beeswax and colophony. However, the protein fraction detected in the adhesive is completely absent from the filler. The precise proportions of each material are difficult to determine,

as the ageing process of some organic compounds might hamper the analysis outcome. For instance, resin components are known to oxidize. The emergence of a range of increasingly polar degradation products affects the chromatographic signal, potencially leading to either a false negative result or a significant underestimation of their concentration [59]. This might very well be the case for colophony, which was detected in very small quantities in the filler and the adhesive. The composition of the binder corresponds to literature on the brocades from the Low Countries [1, 8-10, 15, 19, 20] as previous authors reported the identification by chemical analyses of beeswax as a filler, either alone or in combination with oil and pine resin [1, 8, 9, 15].

The filler also contains pigments, as identified by combined SEM-EDX, FTIR, µRS, and SR-XRPD, with lead white (hydrocerussite and cerussite) as main component in several samples, along with some grains of minium that are heterogeneously dispersed in the reddish part of the layer. SR-XRPD also allowed to detect the presence of lead stearates. Although this interpretation remains hypothetical, the heterogeneous appearance of the filler—characterized by red and white areas (as illustrated in Fig. 6)—may indicate that the presence of lead white was not the result of a deliberate addition by the artist, but rather a possible consequence of the localized degradation of minium. The chemistry involved in the transformation of the lead compounds that may have occurred through natural aging is complex and was discussed elsewhere [60-67]. However, it is well-known that the interaction of minium with oil may lead to the formation of plumbonacrite $3PbCO_3.PbO.Pb(OH)_2$ and consecutively to the formation of hydrocerussite and cerussite as shown by Vanmeert et al. [61] A posteriori the solely identification of the last two compounds mention can bring to the miss-interpretation of a lead white layer while it is actually observed the aging of minium [60-63]. However, its potential transformation is affected by multiple parameters including humidity, light, oxygen, and the presence of atmospheric pollutants (such as SO_2 and CO_2) of which it is not clear to what extent these can reach the filler that is situated relatively deep in the stratigraphy [63, 66-67].

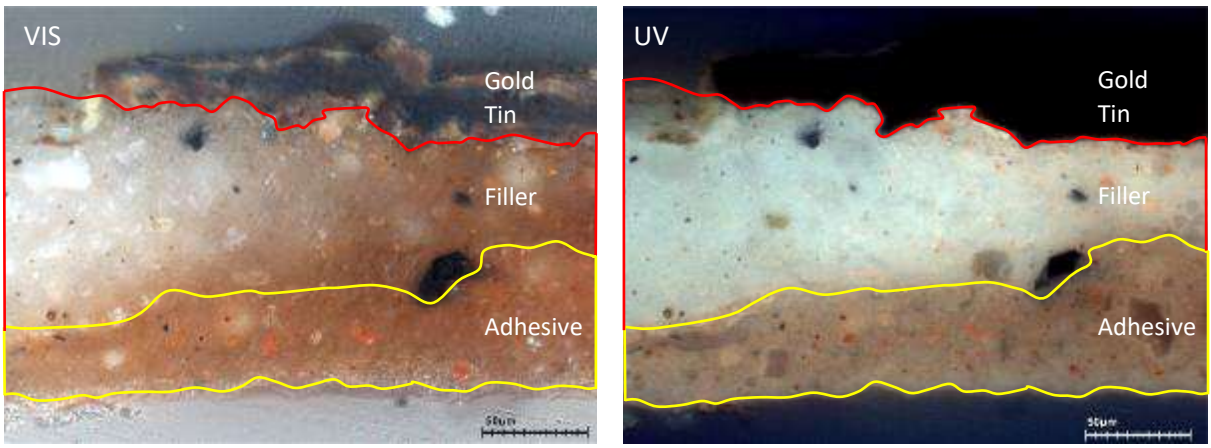


Fig. 6: Micrographs of paint cross-section P.259.024 extracted from the applied brocade on the panel of the Virgin, in normal light (left) and UV light (right) (Magnification X200). The preparatory layers (priming, isolation, ground) as well as the upper parts (paint, non-original varnishes and overpaint) are missing on this sample. The interfaces of the adhesive and the filler are highlighted with yellow and red lines, respectively. The sample location is indicated in Fig. 5.

The adhesion of the gold leaf to the tin foil constitutes a significant aspect of the material composition and technique. Only two from the 12 samples (P259.023 and P033.56, see Fig. 5) exhibited a thin (< 2 µm) mordant layer (layer 7 in Table 1 and Fig. 2) in between the tin foil and the gold leaf, as illustrated by Fig. 7 and 8. It was observed with the upright OM as a fragmentary, translucent layer of which the extreme thinness might have aimed at maintaining the delicate topography of the tin foil [1, 20]. This mordant emerges more clearly in the backscattered electron image (BEI), recorded with FEG-SEM at high magnification (20000x), as a 1-2 µm thick, amorphous layer (Fig. 8c). A point SEM-EDX analysis

(Fig. 8d) revealed the presence of gold, tin and lead. The gold and tin fluorescence signals are originating from the metallic foils applied (tin foil below the mordant and gold leaf above), whereas the detection of lead is considered to be mainly rising from the mordant. Unfortunately, this translucent adhesive layer was too thin to isolate for selective THM-GCMS analyses. The literature available on the topic of gilding on tin describes the use of an oil-based mordant prepared with addition of lead compounds added probably for their oily drying capabilities [1, 27, 68, 69]. For instance, the *Tegernsee Manuscript* (German, ca. 1500*)* describes a recipe with linseed oil and minium to prepare a mordant for gilding on tin, that is consistent with the detection of lead in these layers [27]. Although no discernible pigment grains or particles were found in this sample, a pre-heated oil containing a lead compound may have been used [70, 71], allowing the lead to start reacting with the siccative oil while all the solid leftover has been filtered away.

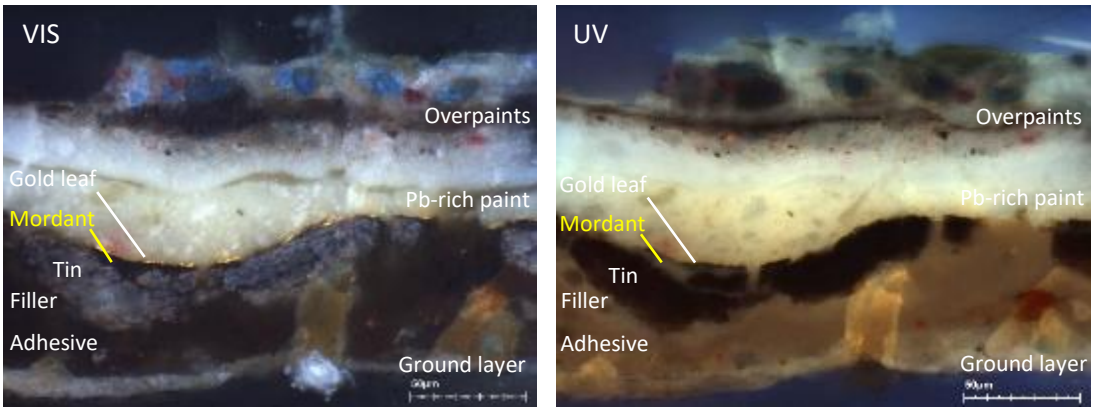


Fig. 7: Micrographs of cross-section (P033.56) extracted from the applied brocade on the panel of the Virgin, in normal light (left) and under UV light (right) (Magnification X200). The sample location is indicated in Fig. 5.

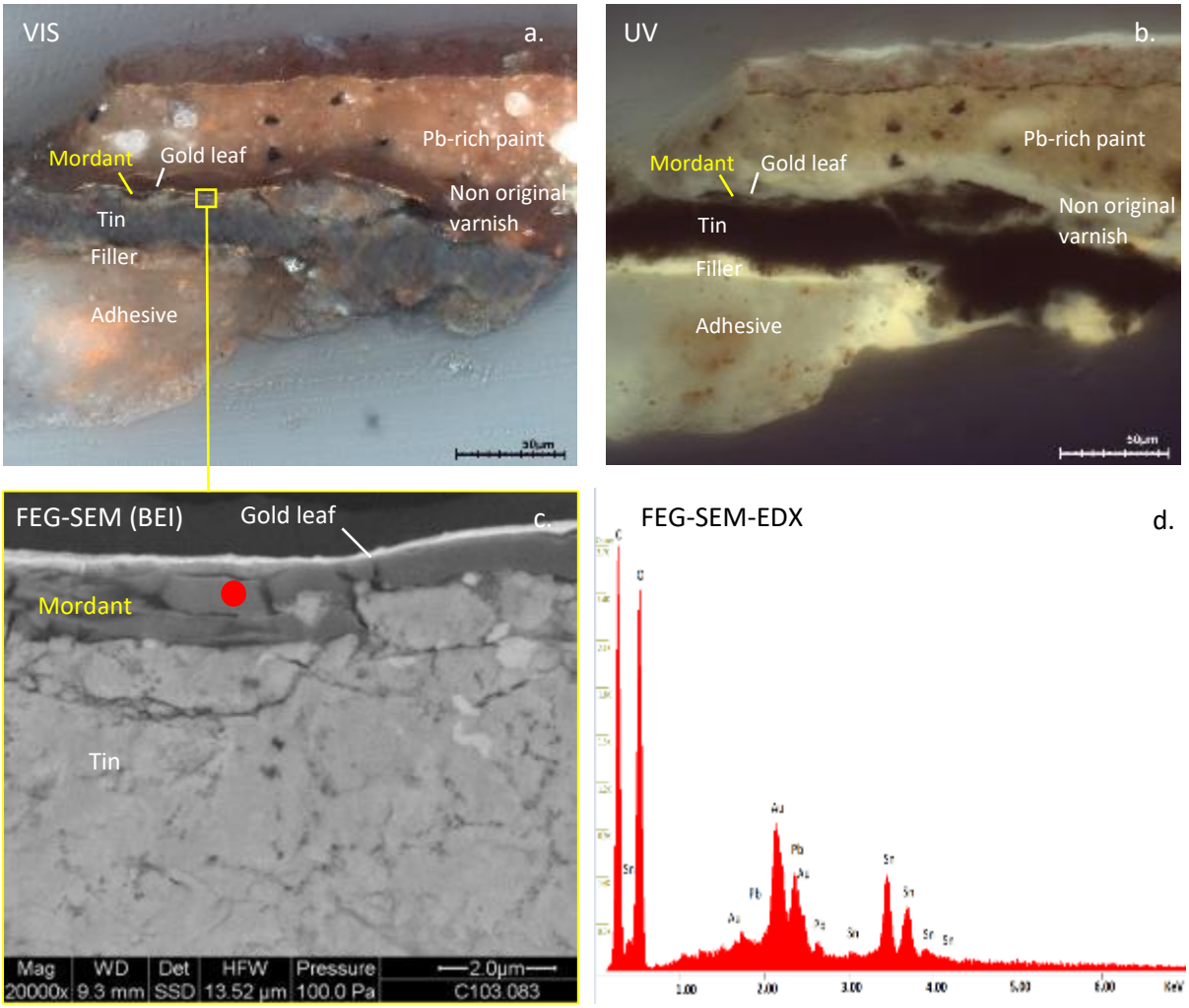


Fig. 8: Top row: Micrographs (magnification X200) of the cross-section P.059.023 extracted from the applied brocade on the panel of the Virgin, in (a) normal light and (b) UV light (the sample location is indicated in Fig. 5). Bottom row: FEG-SEM Backscattered Electron image (10000x) recorded on cross-section P.059.023 (location indicated with a yellow square in fig. 8a). The red spot indicates the location of a point analysis by FEG-SEM-EDX, (d) FEG-SEM-EDX point analysis (indicated by the red spot in Fig.8c) revealing the presence of Au, Pb, and Sn.

Finally, the original paint partially covering the gold leaf (corresponding to layer 9 in Fig. 2) was identified as oil-based with a variety of pigments that are commonly found in paintings of that period in the Low Countries (see Table 1). Over time, various overpaints and varnishes were superimposed during past restoration campaigns; however, these fall outside the scope of this work [2-4].

Degradation of the tin foil

Examination of the samples with upright OM indicates that the tin foils are severely deteriorated. Instead of the anticipated metallic sheen, the tin foils have a heterogenous appearance, locally exhibiting a dark brown, dark grey and/or a whitish grey colour (fig. 9). The thickness of the degraded tin foil ranges between 13 and 20 µm, while the gold leaf thickness was measured to be between 0.10 and 0.16 µm. This difference was expected as, being a less ductile metal than gold, tin could not be beaten as fine as gold leaves. According to literature, tin foil thickness varies between 5 to 80 µm depending on the dexterity of the beater and the type of application for which it is created [1, 17, 72]. However, determining the thickness of tin foils remains challenging, as their thickness most likely increased with the oxidation or phase transformation of the metal [33]. Nevertheless, the tin foils of the Ghent Altarpiece are considered rather thin, as authors previously reported degraded tin foils of

20-50 µm in other artworks from the same period [1, 17, 18]. It is not unthinkable that Van Eyck preferred a very thin foil, as this would have allowed to obtain the particularly refined design of the applied brocades on the altarpiece.

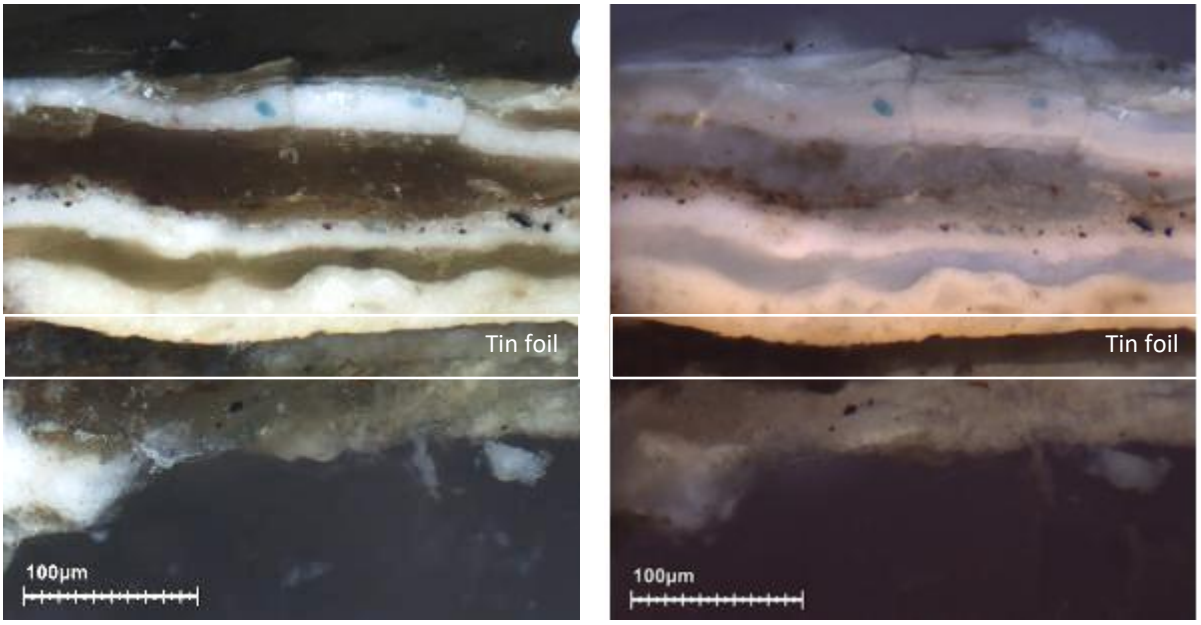


Fig. 9: Micrographs showing cross-section (P033.058) extracted from the applied brocade on the panel of the Virgin, in normal light (left) and UV light (right) (Magnification X200). The location of the tin foil is indicated by a white rectangle. In visible light, the tin foil appears dark on the left part of the image, but white-greyish towards the right side. The sample location is indicated in Fig. 5.

SEM-EDX point analyses conducted on various locations of the degraded tin foil in all 12 cross-sections indicates that the metallic tin used for beating the foil contains a few weight percentages of lead. SEM-EDX analysis also shows a variable amount of oxygen as part of the tin oxides that formed, as well as some chlorine that seems to be bound with lead rather than with tin. The presence of lead in the tin alloy is a significant parameter as this element is known to impact the aging behaviour of tin. For instance, the presence of lead increases the oxidation rate of tin, while it reduces the risk of tin pest formation [21, 29, 33, 38, 41]. However, these results should be interpreted with caution, since factors such as the width of the instrument beam and/or the sample inclination may lead to contributions to the EDX spectra from surrounding lead-rich layers. Nevertheless, synchrotron radiation-based X-ray fluorescence (SR-XRF) conducted on a selection of microsamples (P259.023, P259.024, P259.025, P259.066, P259.067 localised in Fig.5) allowed to confirm the presence of lead in the tin foils, as exemplified in fig.10.

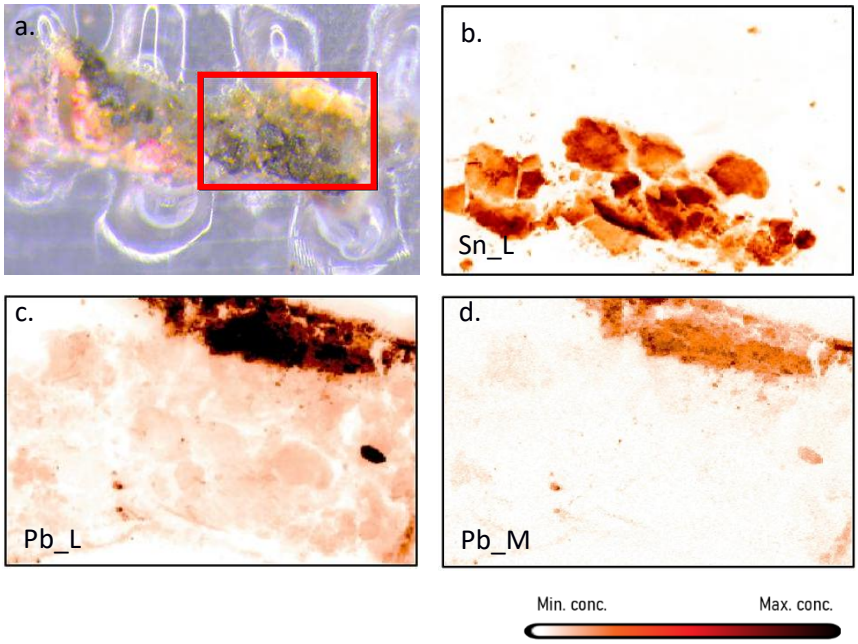


Fig.10: (a) Micrograph showing cross-section (P.033.066) extracted from the applied brocade on the panel of the Virgin (the sample location is indicated in Fig. 5) in VIS light (Magnification X200). The red rectangle indicates the area that was analysed by means of SR-XRF. (b-d) corresponding SR-XRF maps showing the distribution of Sn-L (b), Pb-L (c) and Pb-M (d), indicating the presence of lead in the tin foil. The Pb-rich region observed at the top is attributed to the presence of lead in the filler material adjacent to the tin foil.

In addition, SR-XRPD was conducted on several microsamples (P259.25, P259.23, P033.29, P033.57, sample location is indicated in Fig. 5) in an attempt to obtain a more accurate characterisation of the tin foil. These analyses allowed to provide information regarding the distribution of romarchite (SnO) and cassiterite (SnO_2), detected earlier by MA-XRPD (see p.10). On this selection of microsamples, the SR-XRPD analyses revealed that the metallic tin had fully degraded into SnO and SnO_2 (see fig. 11). These corrosion products are primarily expected to result from the oxidation of the tin foil through contact with the binders in the surrounding layers and exposure to atmospheric oxygen [13, 72]. However, the simultaneous presence of SnO (stannous oxide, Sn(II) and SnO_2 (stannic oxide, Sn(IV)) may also result from more complex chemical pathways occurring within the tin foil [73-78]. In particular, the formation of both oxides could be influenced by the presence of additional tin-containing compounds, such as tin chloride ($SnCl_2$) and/or tin oxalates (SnC_2O_4) [75-76]. Metastable SnO is described in the literature as an intermediate phase in the process of the formation of SnO_2, the most stable and final product of tin oxidation [13, 78]. Thermodynamic considerations derived from archaeological studies of corrosion products on pewter artifacts recovered from marine environments suggest that romarchite, as metastable phase, arises due to sluggish kinetics in the process of the formation of cassiterite (SnO_2) [78 - 80]. These studies further propose that romarchite may form through distinct reaction pathways, depending on the prevailing environmental conditions. In any case, the detection of both romarchite and cassiterite in the tin foils on the Ghent panels after nearly 600 years demonstrates the presence of continuous and complex chemical interactions occurring within the tin foil.

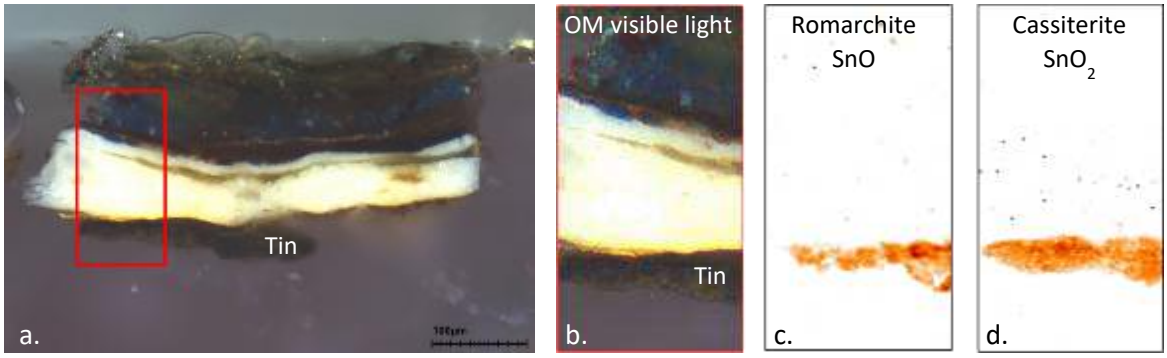
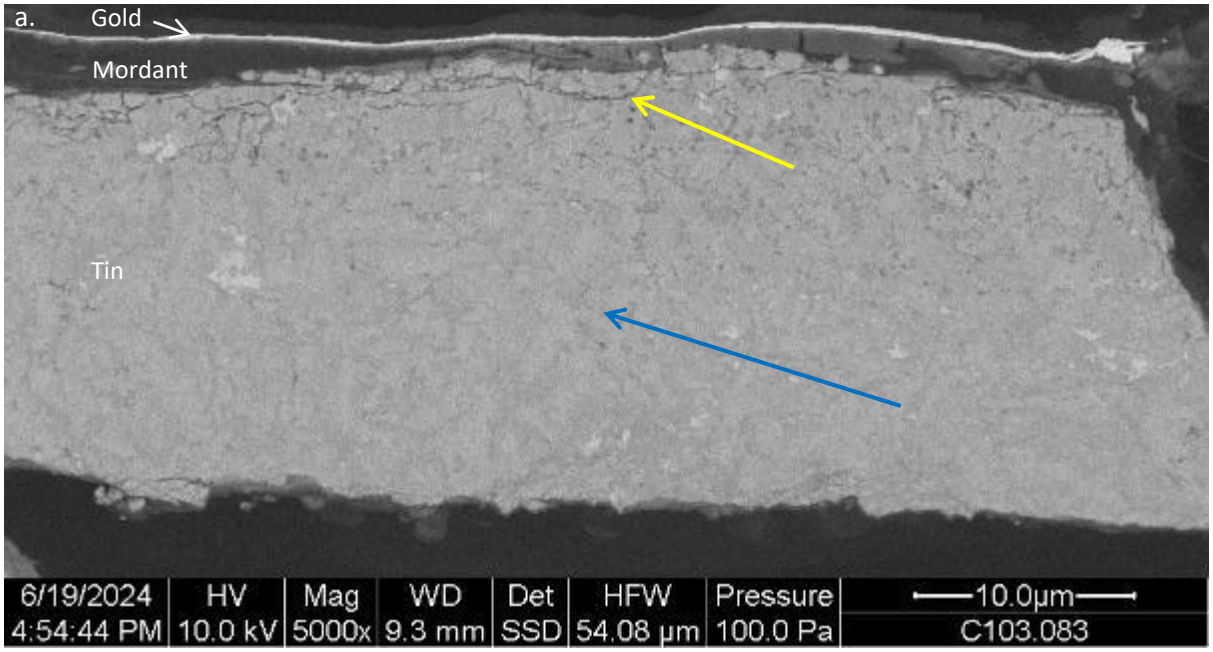


Fig. 11 (a) Micrograph showing cross-section (P.033.057) extracted from the applied brocade on the panel of the Virgin (the sample location is indicated in Fig. 5). Normal light (Magnification X200). The red rectangle indicates the area that was analysed by means of SR-XRPD. (b) Detail of area of the cross section indicated by the red square in Fig. 11a, (c) associated SR-XRPD maps showing the distribution of romarchite (d) and cassiterite.

The microstructure of the tin foil was further characterised with the use of a Field Emission Gun – Scanning Electron Microscope (FEG-SEM), after polishing the samples with ion milling (see Method). The BE images taken at different magnifications (200 to 50000x) illustrate variable condition states of the tin foil. In particular, less-altered tin areas show a porous and compact structure with small fissures (Fig. 12a), while other parts are heavily altered with cracks running through the tin foil either perpendicular with (see yellow arrow in Fig. 12b), or parallel to the surface (see yellow arrow in Fig. 12c). The detachment of micro fragments of tin often occurs around the interface of the foil with the superimposed gold leaf or the underlying filler. In addition, a detachment of the superimposed paint layer is often observed above the gold leaf (see red arrow in Fig. 12c) or the tin foil (in areas where the gold leaf is missing) (see red arrow in Fig. 12b). These degradation processes have rendered the brocades highly fragile, with a loss of cohesion and adhesion of the tin foil. This condition can reasonably be considered to account for the extensive overpainting of the brocade areas.



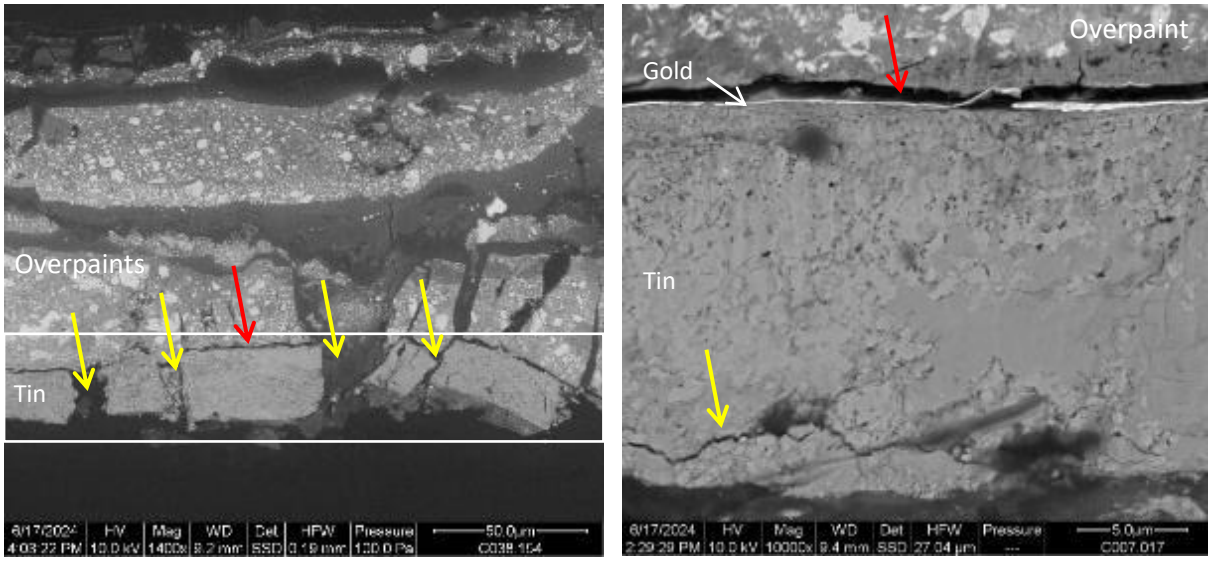


Fig. 12: FEG-SEM BE images illustrating various alterations. (a) FEG-SEM BEI (5000x) of cross-section (P.059.023) extracted from the applied brocade on the panel of the Virgin (the sample location is indicated in Fig. 5). The image shows a relatively well-preserved tin foil with compact structure (blue arrow). Visible alterations are the small fissures visible near the surface of the tin foil, around the interface with the adhesive (mordant) (yellow arrow). (b) FEG-SEM BEI (1400x) of cross-section (P033.055) extracted from the applied brocade on the panel of the Virgin (the sample location is indicated in Fig. 5). The image shows a tin foil broken up by large perpendicular cracks (yellow arrows). A delamination of the upper paint layer is also visible above the tin foil (red arrow). (c) FEG-SEM BEI (10000x) of cross-section (P033.058) extracted from the applied brocade on the panel of the Virgin (See Fig. 5 for the sample location). The image shows a tin foil with a crack running parallel with and near (yellow arrow) the interface with the filler (bottom edge). This almost leads to the detachment of a micro-fragment of tin. A crack between the gold leaf and the superimposed paint layer is also visible (red arrow).

An interesting phenomenon was observed in the layers below the tin foil, i.e. the filler and the adhesive, in which very small and dispersed aggregates of tin were detected with FEG-SEM (Fig. 13). These tin aggregates seem to adhere as a film around the walls of the cavities present in the filler and adhesive, which are both rich in organic binder (fig. 13a-c). Their presence in these layers raises the question whether the formation of organo-tin products (e.g. tin soaps) can result from the reaction of the tin foil in contact with the oil-resinous-wax matrix [81-84]. If formed, these tin compounds could then migrate and accumulate in pre-existing pores in the adhesive and filler.

To test this hypothesis, O-PTIR analysis were performed on the areas containing tin aggregates (Figure 13d). O-PTIR is a recently developed technique that provides spectra comparable to FTIR in transmission mode, with a spatial resolution of 0.5 µm, which has been successfully applied to the characterization of small particles and thin layers of paintings samples [85, 86]. In order to avoid potential radiation damage induced by the SEM-EDX maps, a nearby area showing the same features was analysed. As it can be observed, the spatial distribution of the Sn aggregates is correlated with two broad absorption peaks cantered at around 1630 and 1385 cm^{-1}: these peaks fall within the spectral regions of the asymmetric and symmetric vibrations of carboxylates, typically detected in mixtures of linseed oil with metallic ions [87, 88]. Given that only Sn (and small amounts of Si) are present in this area (Fig.13c), the results suggest the formation of Sn carboxylates. However, the unambiguous identification of these compounds would require a more dedicated study, including the analysis of pure reference materials and additional high-spatial-resolution data from the interface between the binding medium and the tin foils.

Literature on this topic is in fact very scarce, but a recent study by Biocca did demonstrate the production of tin metal soaps due to interactions between tin foils and the fatty acids present in the

oil-resinous-wax based adhesive mixture of artificially aged mock-ups [81]. According to Biocca, these chemical interactions would be promoted by humidity and variations of temperature [81, 82]. In addition, the same author confirmed, for the first time, the presence of tin soaps in tin-based decorations on artworks, i.e. on the fresco *Vela Della Castita* (Basilica of Saint Francis in Assisi) and the Giotto *Universal Judgement* (Scrovegni Chapel in Padua) [81]. It is not impossible that similar reactions occurred on the applied brocades of the Ghent Altarpiece since similar materials are encountered.

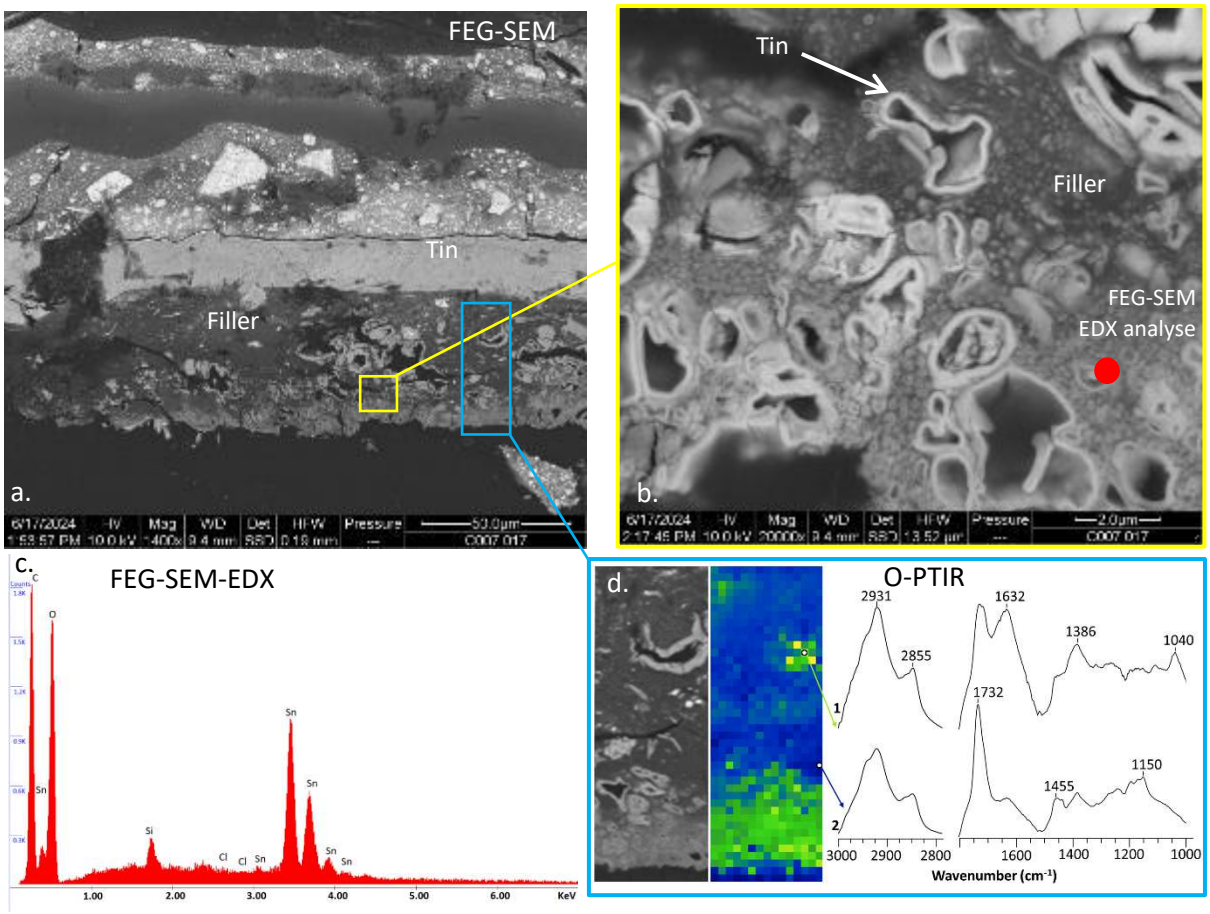


Fig. 13: (a) FEG-SEM BEI (1400x) of cross-section (P033.058) extracted from the applied brocade on the panel of the Virgin (the sample location is indicated in Fig. 5). The yellow square indicates the detailed area (higher magnification) shown in Fig.13b, the blue square indicates the area analyzed with O-PTIR in Fig.13d; (b) FEG-SEM BEI (20000x) of cross-section (P033.058). The 'white rims' that seem to coat the edges of (or fill) the pores of the oil-, wax-, and resin-based filler contain tin. The location of the point EDX analysis shown in Fig 13c, is indicated by the red spot. (c) FEG-SEM EDX point analysis indicates the presence of tin. (d) O-PTIR multispectral imaging analysis (map size: 41 µm x 15 µm, pixel size: 1 µm x 1 µm): integration map of the spectral region corresponding to the markers tentatively assigned to tin carboxylates (1670-1570 cm^{-1}) and representative spectra of (1) carboxylates potentially formed with tin and (2) organic binder.

Finally, the FEG-SEM images taken from several samples (P033.058, P259.024, P259.025, localised in Fig. 5) highlight yet another compelling alteration phenomenon at the interface between the tin foil and the gold leaf. The gold leaf takes a tooth-like shape at the interface between Au/Sn as if both metal foils dissolve into each other (Fig. 14, indicated by the yellow arrows). In fact, this degradation shows strong resemblance to a mechanism that is well-known in metallography: the dissolution of metallic gold in tin [89-93]. This process may occur over a long period of time when Au^0 is in contact with $Sn^0$and it is known to be accelerated by heating. The two layers interact to form intermetallic

compounds and alloy such as: $AuSn_4$, $AuSn_2$ or AuSn at their interface [89-93]. This interaction between tin and gold, coupled with the degradation of the tin foil itself, could be the reason why the fine mordant film in between both metal layers is no longer visible in most of the samples analysed.

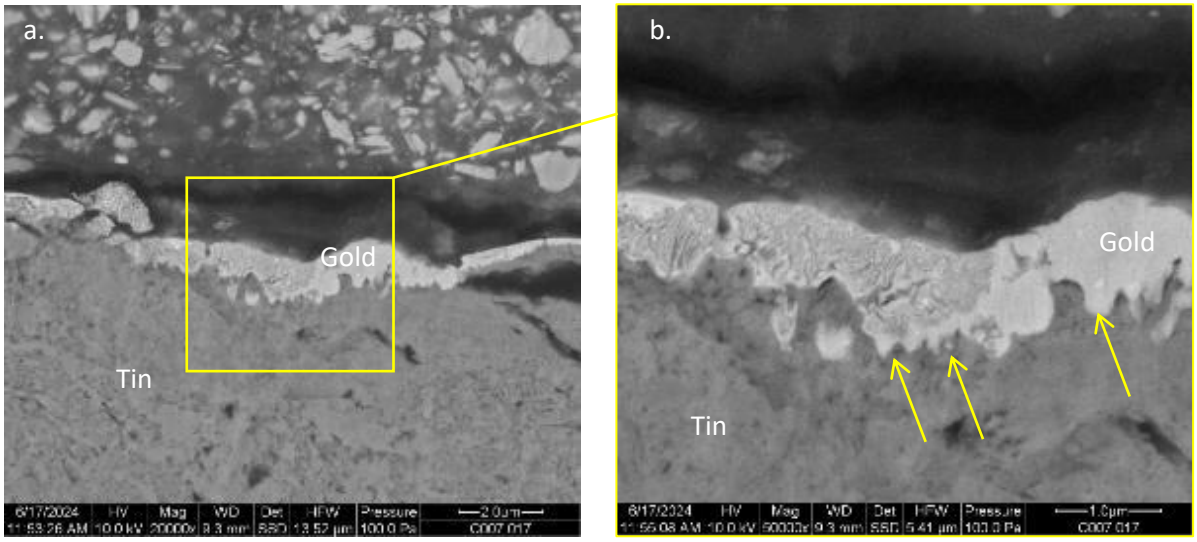


Fig. 14: (a) FEG-SEM BE image (20000x) of cross-section (P033.058) extracted from the applied brocade on the panel of the Virgin (the sample location is indicated in Fig. 5). The yellow square indicates the detail shown in fig. 14b. (b) FEG-SEM BE image (20000x) of cross-section (P033.058). The yellow arrows indicate the "teeth" like structure in the gold leaf, at the interface with tin.

CONCLUSION

Combining careful visual inspection of the panels with in situ non-invasive analyses by MA-XRF/MA-XRPD and chemical analyses of samples by SEM-EDX, FTIR, µRS, THM-GCMS, FEG-SEM, O-PTIR, SR-XRF and SR-XRPD, was a successful approach to characterise the applied brocades of the Ghent Altarpiece. As exemplified by the Saint John detail, the MA-XRF scans proved particularly useful to provide information regarding the nature of the materials, to assess the general conservation state of the applied brocades, to localise several past interventions (overpaints, filling, regilding, etc.) and to determine the most suitable areas for collection of microsamples. The latter was necessary to obtain a more accurate characterisation of the materials and a better understanding of the general structure of the applied brocades. Furthermore, this study highlighted degradation phenomena. The tin has largely transformed into the corrosion products romarchite (SnO) and cassiterite (SnO_2), accompanied by extensive cracking, loss of cohesion and delamination at the interfaces between/ within the filler, gold leaf, and paint layers. Additional alteration phenomena include the possible formation of organo-tin compounds within the organic layers and intermetallic interactions between gold and tin, contributing to the disappearance of the original mordant and further destabilisation of the stratigraphy. Both these phenomena were rarely observed and investigated on applied brocades. So far, numerous papers have been published on the degradation of objects made of tin (such as crockery and organ pipes), but literature is very scarce on the degradation of gilded tin foils in contact with paint layers. This study clarified that future work should focus on potential interactions between tin foils and organic binders (e.g. the formation of organotin compounds such as tin soaps), and assess their role in brocade deterioration. In addition, the possible transformation of minium into lead white in the filler layer and its impact on the stability and alteration of the overlying tin foil is another aspect that merits further study.

Acknowledgments

The authors acknowledge the team of conservators of the Ghent Altarpiece for their remarks and precious feedback, in particular Marie Postec, Griet Steyaert, Nathalie Lacquière, Laure Mortiaux, and Cécile de Boulard. The authors also wish to express their gratitude to Patrick Storme for sharing his valuable expertise on metal foils. We acknowledge DESY (Hamburg, Germany), a member of the Helmholtz Association HGF, for the provision of experimental facilities. Parts of this research were carried out at P06. Data was collected using the Micro X-ray diffraction station operated/provided by DESY Photon Science. We would like to thank Jan Garrevoet, Ken Vidar, and Dennis Brückner for assistance during the experiments. Beamtime was allocated for I-20240920 EC. We acknowledge the European Synchrotron Radiation Facility for provision of synchrotron radiation facilities and we would like to thank for assistance in using beamline ID13/ID22 through the historical materials BAG access HG-237. As well, the authors acknowledge Synchrotron SOLEIL (Gif-sur-Yvette, France) for the fundings received to perform O-PTIR analyis (Beamtime proposal number 20241752). Sincere thanks also go to Teresa Scovacricchi, for her assistance during the sample preparation and the measurements. V.B. and A.M. acknowledge FEDtWIN program from Belspo for funding the project EPITOX#2 (Prf-2021-007) and BELCAIRE (Prf- 2021-041). A.R-C. and A.K. acknowledge the Fonds Wetenschappelijk Onderzoek (FWO) for funding grants 1183125N and G060422 N, respectively. Finally, sincere thanks are extended to the Gieskes Strijbis fund for their generous support.

Declaration of competing interest

The authors declare that they have no known competing financial interests or personal relationships that could have appeared to influence the work reported in this paper.

Credits

S.K. wrote the main manuscript text which was revised and corrected by her supervisors G.V.d.S., J.S., K.J. and H.D. who also helped with conceptualizing the paper, interpreting data and secure funding. As an expert in applied brocades, I.G. assisted with the material-technical interpretation of the data. M.K., C.B., C.G., M.S. and L.D. assisted with sample preparation, recording OM micrographs and SEM measurements. A.R-C., A.K. and S.K. carried out MA-XRF imaging experiments and processed the data. S.D.M. performed MA-XRPD and data processing. E.C.A. and S.D.M. performed SR-XRPD and SR-XRF analysis at synchrotron end station, as well as data processing, while A.M., V.B. and F.B. performed O-PTIR and processed the ensuing data.

REFERENCES

1. Geelen, I., and Steyaert, D., *Imitation and Illusion. Applied Brocade in the Art of the Low Countries in the Fifteenth and Sixteenth Centuries.* Scientia Artis, 6, 2011.
2. Coremans, P. *L'Agneau mystique au Laboratoire. Examen et traitement.* Contributions à l'étude des Primitifs flamands, 2, 1953.
3. Dubois, H., "The conservation history of the Ghent Altarpiece", in the Burlington magazine, 160, 2018, p. 754-765
4. Sanyova, J., Van der Snickt, G., Dubois, H., Coudray, A., Janssens, K., Vandenabeele, P., "Paint and Polychromy: Chemical Investigation of the Overpaints", *The Ghent Altarpiece Research and Conservation of the Exterior*, in *Contributions to the Study of the Flemish Primitives*, Fransen, B., Stroo, C. (Eds), Royal Institute for Cultural Heritage, 2020, p. 77-109

5. Brinkman, P.W.F., Kockaert, L., Maes, L., Thielen, E.M.M., and Wouters, J., "Het LamGodsretabel van Van Eyck. Een heronderzoek naar de materialen en schildermethoden, 2. De hoofdkleuren. Blauw, groen, geel en rood", Koninklijke Instituut voor het Kunstpatrimonium, Bulletin 22, 1988-1988, p. 26-50
6. Van der Snickt, G., Dooley, K. A., Sanyova, J., Dubois, H., Delaney, J.K., Gifford, E.M., Legrand, S., Laquiere, N., and Janssens, K., "Dual mode standoff imaging spectroscopy documents the painting process of the Lamb of God in the *Ghent Altarpiece* by J. and H. Van Eyck", *Sciences Advances,* 2020, 6
7. Van der Snickt, G., Dubois, H., Sanyova, J., Legrand, S., Coudray, A., Glaude, C., Postec, M., Van Espen, Piet., Janssens, K., "Large-Area Elemental Imaging Reveals Van Eyck's Original Paint Layers on the Ghent Altarpiece (1432), Rescoping Its Conservation Treatment", Angewandte Chemie International Edition, 56, p. 4797-4801
8. Darrah, J., "White and Golden Tin Foil in Applied Relief Decoration: 1240-1530", in *Looking through paintings: The study of painting techniques and materials in support of art historical research,* Hermens, E., (Ed.), Archetype Publications, 1998, p. 49-79
9. Martinetto, P., Blanc, N., Bordet, P., Champdavoine, S., Fabre, F. , Guiblain, T., Hodeau, J.-L., Lelong, F., Leynaud, O., Prat, A., Pouyet, E., Uher, E. , Walter, Ph., "Non-invasive X-ray investigations of medieval sculptures: New insights on "applied tin-relief brocade" technique, Journal of Cultural Heritage, 47, 2021, p. 89-99
10. Nadolny, J., *The techniques and use of gilded relief decoration by northern European painters, c.1200-1500*, Thesis dissertation, Courtauld Institute of Art, 2000
11. Mounier, A., Daniel, F., "Sgraffito, zwischgold et brocart appliqué La dorure dans tous ses états au sein de quelques peintures murales (XIe-XVIe siècle) du Sud-Ouest de la France", ArcheoSciences, revue d'archéométrie, 37, 2013, p. 33-40
12. Rodriguez-lopez, A., Bazeta Gobantes, F., "Applied brocade in Spain Origin, making procedures and designs in Northern Spain", CeRoArt, Vol.HS, 2021
13. Szmelter, I., Walter, P., Rousselière, H., "New Information Provided by Multidisciplinary and Combined Studies, Including Radiography, XRD and XRF, of the triptych the Last Judgement from National Museum in Gdańsk: Rogier van der Weyden and Hans Memling co-authorship", Opuscula Musealia, 23, 2015, p. 61-73
14. Betts, P., and Gates, G., "Dressed in Tin: Analysis of the Textiles in the Abduction of Helen Series", The Walters Art Museum, 74, 2019, p.1-44
15. Von Baum, K., Dietemann, P., Fischer, U., Klein, P., Krischel, R., Neuhoff, T., Von Saint-George, C., Schaefer, I., Schawe, M., Stege, H., Walcher, J., *Let the Material Talk, Technology of Late Medieval Cologne Panel Painting,* Archetype Publications, 2014
16. Volk, A., "An Eventful History. The Crucified Thief Examined and Restored*",* in *With New Splendour. The Crucified Thief by the Master of Flémalle in Context*, Schnell+Steiner, 2017, p 39-75.
17. Roberto Amieva, C., *Brocade applied in Aragon. Sources, typologies and technical aspects,* Thesis Dissertation, University of Sevilla, 2013.
18. Barrio Olano, M., and Berasain Salvarredi, I., "Applied-brocade in the altarpiece of the *Coronation of the Virgin* of Errenteria, Basque Country"**,** in *Polychrome Sculpture: Decorative Practice and Artistic Tradition,* S. Litjens, K. Seymour (Eds.), 2017, p. 106–115
19. Massing, A. (Ed), *The Thornham Parva retable : technique, conservation and content of an English medieval painting*, Whittlesford, Cambridge : Hamilton Kerr Institute, University of Cambridge, Harvey Miller, 2003
20. Da Silva, A., "Reconstruction of the tin relief decoration on the Thornam Parva Retable", in Artist's Footsteps: the reconstruction of pigments and paintings, Archetype publication, 2012.

21. Cardell, C., Guerra, I., Yebra-Rodriguez, A., “Tin Deterioration on Polychrome Stone Sculptures of the San Jerónimo Church (Granada, Spain), Revista de la Sociedad Española de Mineralogía, 2012, p. 1-2
22. Cavallo, G., Verda, M., “Historical, Mycroanalytical Evidences and Limits of Non Invasive Technologies in Studying Gildings on 16th c. Wall Paintings”, 9th International Conference on NDT of Art, Jerusalem Israel, 25-30 May 2008, 2008, p. 1-5
23. Rodriguez-Lopez, A., Bazeta Gobantes, F., “Classification of the Typologies, Techniques and Materials of the Applied Brocades of the Altarpieces of Gipuzkoa by Means of the Analytical Techniques of Laboratory”, 9th International Conference on NDT of Art, Jerusalem Israel, 25-30 May 2008, 2008, p. 1-10
24. Serandan, C., Hradilová, J., Hradil, R.,“The Imitation of Brocade Fabrics in Late Medieval Altarpieces from Transylvania”, Acta Artis Academia, 2010, p. 42-62
25. Lelong, F., Pouyet, E., Champdavoine, S., Guiblain, T., Martinetto, P., Walter, P., Rousselière, H., Cotte, M., “Des « brocarts appliqués » dans la sculpture savoyarde Vers une caractérisation interdisciplinaire”, CeRoArt, Vol.HS, 2021
26. Cennino Cennini, *Il Libro Dell’arte, Le Livre de l’art,* Translation by Colette Déroche, Berger-levrault, Paris, 1991
27. Anonymous, *Tegernsee Manuscript* or *Liber Illuministrarum*, *Library of the State of Bavaria in Munich (cod. germ. 821),* Edition: Bartl, Krekel, Lautenschlager, and Oltrogge 2005: 284-285, No. 683
28. Fücker, B., Kramer, J., Dietemann, P., and Stege, H., “News from Tegernsee: The Tegernsee Tabula Magna and the Liber Illuministarum revisited”, ICOM-CC publication online, Art Technological Source Research 9, Paris, 2022, p.9-19
    https://www.icom-cc-publications-online.org/5962/News-from-Tegernsee--The-Tegernsee-Tabula-Magna-and-the-Liber-illuministarum-revisited
29. Scott, D., *Metallography and Microstructure of Ancient and Historic Metals*, Getty Conservation Institute in association with Archetype Book, 1991
30. Chiavari, C. Martini, C. Poli, G. and Prandstraller, D., “Deterioration of tin-rich organ pipes.” Journal of Materials and Sciences, 41, 2006, p. 1819-1826
31. Plumbridge, W. J, “Further observations on tin pest formation in solder alloys”, Journal of Electronic Materials, 39, 2010, p.433-440
32. Joo, Y.J., Takemoto T., “Transformation of Sn–Cu alloy from white tin to gray tin”, Materials Letters, 56, 2002, p. 793-796
33. Steyaert, D., and Sanyova, J., “Matériaux et structure des “brocarts appliqués” dans les anciens Pays-Bas méridionaux, synthèse d’une recherche approfondie”, Ce ROArt, HS, 2021
34. Duran, A., Perez-Rodriguez, J.L., Jimenez de Haro, M.C., Justo, A., “Degradation of gold and false golds used as gildings in the cultural heritage of Andalusia, Spain”, Journal of Cultural Heritage, 9, 2008, p. 184-188
35. Crina Anca Sandu, I., M., de Sa, and Pereira, M., "Ancient ‘gilded’ art objects from European cultural heritage: A review on different scales of characterization”, Surface and Interface Analysis, 43, 2011, p. 1134-1151
36. Pinto, A., Poline, V., Bouvier, C., Bordet, P., Blanc, N., Fabre, F., Lelong, F., Martinetto, P., "The degradation of metal sheets in polychrome sculpture: the «applied brocades» of Savoy”, *ArcheoSciences* [Online], Vol. 47-1, 2023, p. 79-92
37. Lyon, S., Richardson, T., Cottis, B., Lindsay, R., Scantleburry, D., Graham, M., Stott, H., “Corrosion of Tin and its Alloys”, In *Shreir's Corrosion: Volume 3: Corrosion and Degradation of Engineering Materials* Elsevier BV.

38. Ospitali, F., Chiavari, C., Martini, C., Bernardi, E., Passarini, F., Robbiola, L., "The characterization of Sn-based corrosion products in ancient bronzes: a Raman approach", Journal of Raman Spectroscopy, 43, p. 1523-1844
39. Bovelacci, A., Ciliberto, E., Greco, E., Viscuso, E., "Surface and Bulk Investigations of Organ Metal Pipe Degradation", in Youth in Conservation of Cultural Heritage, YOCOCCu 2012, Procedia Chemistry, 8, 2013, p. 130-138
40. De Ryck, I., Van Biezen, E., Leyssens, K., Adriaens, A., Storme, P., Adams, F., "Study of the Corrosion: The Influence of Alloying Elements", Journal of Cultural Heritage, 5, 2004, p. 189-195
41. Peng, W., "An Investigation of Sn Pest in Pure Sn and Sn-based Solders", Microelectronics Reliability, 49, 2009, p. 86-91
42. Matvienko, A.A., Sidelnikov, A.A., "The Influence of Relaxation of Stresses Occurring During the ß -> a Transformation of Tin on the Kinetics of the Transformation", Journal of Alloys and Compounds, 252, 1997, p. 172-178
43. Van der Snickt, G., Miliani, C., Janssens, K., Brunetti, B., Romani, A., Rosi, F., Walter, P., Castaing, J., De Nolf, W., Klaassen, L., Labarque, I., and Wittermann, R., "Material analyses of 'Christ with singing and music-making Angels', a late 15th-C panel painting attributed to Hans Memling and assistants: Part I. non-invasive in situ investigations", Journal of Analytical Atomic Spectrometry, 11, 2011, p. 2216-2229
44. Alfeld, M., Janssens, K., Dik, J., Nolf, W., and van der Snickt, G., Optimization of mobile scanning macro-XRF systems for the *in situ* investigation of historical paintings, journal of Analytical Atomic Spectrometry, 2011, p. 899-909
45. Deleu, N., Hillen, M., Steenackers, G., Borms, G., Janssens, K., Van der Stighelen, Van der Snickt, G., "Combined Macro X-ray Fluorescence (MA-XRF) and Pulse Phase Thermography (PPT) Imaging for the Technical Study of Panel Paintings", Talanta, 270, 125533
46. Da Silva, A., Legrand, S., Van der Snickt, G., Featherstone, R., Janssens, K., Botinelli, G., "MA-XRF imaging on René Magritte's La Condition Humaine: insight into the artist's palette and technique and the discovery of a third quarter of la Pose enchantée", Heritage Science, 2017.
47. Vanmeert, F., De Nolf, Wout, De Meyer, S., Dik, J., and Janssens, K., "Macroscopic X-ray powder diffraction scanning - a new method for highly selective chemical imaging of works of art: instrument optimization", Analytical Chemistry, 90, 11, 2018, p. 6436–6444
48. De Nolf W, Vanmeert F, Janssens K., "XRDUA: crystalline phase distribution maps by two-dimensional scanning and tomographic (micro) X-ray powder diffraction", J. App.l Crystallogr., 47, 2014, p. 1107–17.
49. Sanyova, J., Van der Snickt, G., Mederos-Henry, F., "The Challenge of a Complex Stratigraphy from a Chemical Point of View", in The Ghent Altarpiece Research and Conservation of the Interior: The Lower Register", The Royal Institute for Cultural Heritage, 2021, p.111-148.
50. Eveno, M., Ravaud, E., Calligaro, T., Pichon, L., Laval, E., "The Louvre Crucifix by Giotto – Unveilling the Original Decorations by 2D-XRF, X-Ray Radiography, Emissiography, and SEM-EDX Analysis", Heritage Science, 2014, p. 2-17
51. Osticioli, I., Lavacchi, A., Capozzoli, L., Berreti, E., Gallo, L., Berberich, C., Agresti, J., Siano, S., "Novel Insights on the Study of a Fifteenth-century Oro di Metà/Zwischgold Gilding by Means of Ion and Electron Microscopy: Characterisation of the Stratigraphy Avoiding Cross-section Preparation", Journal of Cultural Heritage, 44, 2020, p. 297-306
52. Cotte, M., Gonzalez, V., Vanmeert, F., Monico, L., Dejoie, C., Burghammer, M., Huder, L., de Nolf, W., Fisher, S., Fazlic, I., et al. "The "Historical Materials BAG": A New Facilitated Access to Synchrotron X-ray Diffraction Analyses for Cultural Heritage Materials at the European Synchrotron Radiation Facility", *Molecules*, Vol. 27(6), 2022.

53. Riekel, C., Burghammer, M., and Davies, R., “Progress in micro- and nano-diffraction at the ESRF ID13 beamline”, Materials Science and Engineering, Vol. 14, 2010, p.1-9.
54. Schroer, C. G. ; Boye, P. ; Feldkamp, J. M. ; Patommel, J. ; Samberg, D. ; Schropp, A. ; Schwab, A. ; Stephan, S. ; Falkenberg, G. ; Wellenreuther, G. ; Reimers, N. : Hard X-ray nanoprobe at beamline P06 at PETRA III. *Nuclear instruments & methods in physics research* A 616, 2010, p.93-97
55. M. Toplak, G. Birarda, S. Read, C. Sandt, S. M. Rosendahl, L. Vaccari, J. Demšar, F. Borondics, “Infrared Orange: Connecting Hyperspectral Data with Machine Learning”, Synchrotron Radiation News, 30, 2017, p. 40–45.
56. Demšar, J., Curk, T., Erjavec, A., Gorup, Č., Hočevar, T., Milutinovič, M., Možina, M., Polajnar, M., Toplak, M., Starič, A., Štajdohar, M., Umek, L., Žagar, L., Žbontar, J., Žitnik, M., Zupan, B., “Orange: Data Mining Toolbox in Python”, Journal of Machine Learning Research, 14, 2013, p. 2349–2353.
57. Feller, R., *Artists’ Pigments: A handbook of their History and Characteristics*, Archetype Publication 1, 1986.
58. Eastaugh, N., Walsh, V., Chaplin, T., Siddall, R., *The Pigment Compendium: A dictionary of Historical Pigments*, 2004
59. Scalarone, D., Lazzari, M., Chiantore, O., “Ageing behaviour and pyrolytic characterisation of diterpenic resins used as art materials: colophony and Venice turpentine”, Journal of Analytical and Applied Pyrolysis, 64, 2002, p.345–361
60. Cotte, M. et al., “Lead soaps in paintings: Friends or foes?”, Studies in Conservation. 2016; Vol. 62, p. 2-23.
61. Vanmeert, F., Van der Snickt, G., Janssens, K., “Plumbonacrite Identified by X-ray Powder Diffraction Tomography as a Missing Link During Degradation of Red Lead in a Van Gogh Painting”, in Angewandte Chemie, 54, 2015, p. 1-5
62. Keune, K., Van Loon, A., Boon, J.J., “SEM Backscattered-Electron Images of Paint Cross Sections as Information Source for the Presence of the Lead White Pigment and Lead-Related Degradation and Migration Phenomena in Oil Paintings”, Microscopy and Microanalysis, 17, 2011, p. 696-701
63. Aze, S, « Altérations chromatiques des pigments au plomb dans les œuvres du patrimoine, Etude expérimentale des altérations observées sur les peintures murales », PhD Thesis, Université de droit, d’économie et des sciences, 2005.
64. Mecklenburg, M., Tumosa, C., and Vicenzi, E., “The influence of pigments and metal ions on the durability of drying oil and alkyd paints”, in *New Insight into the Cleaning of Paintings, Proceedings from the Cleaning 2010 International Conference*, Smithsonian Institution, 2010, p.59-67
65. Cotte, M., Checroun, E., Susini, J., Walter, P., “Micro-analytical study of interactions between oil and lead compounds in painting”, Applied Physics A, 89, 2007, p. 841-848
66. Hermans, J., Keune, K., van Loon, A., Iedema, P., “The crystallization of metal soaps and fatty acids in oil paint model systems”, Physical Chemistry Chemical Physics, 18, 2016, p. 10896 – 10905
67. Casadio F, Keune K, Noble P, Van Loon A, Hendriks E, Centeno SA, Osmond G, (Eds.). *Metal soaps in art: conservation and research*. Cultural Heritage Science. Cham, Springer International Publishing. 2019, 594 p.
68. Neven, S., The Strasbourg Manuscript, A Medieval Tradition of Artists’ Recipe Collections (1400-1570), Archetype Publication, London. 2016.
69. Anonymous, Paris, Bibliothèque Nationale de France Ms. Fr. 640: 7r, (BNF 640, French, late sixteenth century). Edition and translation: Making and Knowing. November 21 2024, https://edition640.makingandknowing.org/#/folios
70. Kirkpatrick, S., Sanyova, J., Janssens, K., Van der Snickt, G. “The synergistic influence of metal cations on the drying and viscosity of linseed oil assessed by means of model samples containing synthesised metal carboxylates”, Heritage science, 12, 2024, p. 1-15

71. De Viguerie, L., Payard,P.A., Portero, E., Walter, P., Cotte, C., “The drying of linseed oil investigated by Fourier transform infrared spectroscopy: Historical recipes and influence of lead compounds”, Progress in Organic Coatings, Elsevier, 2016, 93, p. 46-60.
72. Nadolny, J., “Some Observations on Northern European Metal beaters and Metal Leaf in the Late Middle Ages.”, in *The Materials, Technology, and Art of Conservation: Studies in Honor of Lawrence J. Majewski on the Occasion of His 80th Birthday, February 10, 1999,* Rushfield, R., and Ballard, M. (Eds.), Conservation Center of the Institute of Fine Arts, New York University, 1999, p. 134-136
73. Campo, C., Rodríguez, J., Ramírez, A., “Thermal behaviour of romarchite phase SnO in different atmospheres: a hypothesis about the phase transformation”, Heliyon, Vol.2 (5), 2016
74. Sarker, P., Huda, M., “Understanding the thermodynamic pathways of SnO-to-SnO_x phase transition”, Computational Materials Science, Vol. 111, 2026, P. 359-365
75. Deng, H., Lamelas, F., Hossenlopp, J., “Synthesis of Tin Oxide Nanocrystalline Phases Via Use of Tin (II) Halide Precursors”, Chemistry Faculty Research and Publications, Vol. 15, 2003
76. Taib, H., Sorrel, C, “Synthesis of Tin Oxide (SnO2) by the Oxalate Route: Effects of Addition Method and Ageing”, Material Science Forum, 2007, p. 973-976
77. Berger, D., Soles, J., Giumlia-Mair, A., Brügmann, G., Galili, E., Lockhoff, N., Pernicka, E., “Isotope systematics and chemical composition of tin ingots from Mochlos (Crete) and other Late Bronze Age sites in the eastern Mediterranean Sea: An ultimate key to tin provenance?”, PLoS ONE, Vol. 14(6), 2019
78. Dunkle, S. E., Craig, J. R., Rimstidt, J. D., and Lusardi, W. R.: Romarchite, hydroromarchite and abhurite formed during the corrosion of pewter artifacts from the Queen Anne's Revenge (1718), Can. Mineral., 41, 659–669, 2003.
79. 85 Dunkle, S. E. (2002): *Romarchite and Other Corrosion Phases on Metal Artifacts from the Queen Anne’s Revenge (1718).* Master Thesis, Virginia Polytechnic Institute and State University, 56 pp. [http://hdl.handle.net/10919/31933]
80. 86 Stacie E. Dunkle, James R. Craig, Wayne R. Lusardi :*Romarchite and associated phases as common corrosion products on pewter artifacts from marine archaeological sites,* 2004 https://doi.org/10.1002/gea.20009
81. Biocca, P., *Metals and Organic Materials in the Cultural Heritage Field: an Approach Through Secondary Ion Mass Spectrometry,* PhD Thesis, Dottorato di Ricerca in Elettronica Applicata, Roma Tre University, 2018.
82. Casadio F, Keune K, Noble P, Van Loon A, Hendriks E, Centeno SA, Osmond G. Metal soaps in art: conservation and research cultural heritage science. Cham: Springer International Publishing; 2019.
83. Hermans, J.J., Metal soaps in oil paint: structure, mechanisms and dynamics, PhD Thesis, Universiteit van Amsterdam. 2017; 168
84. Garrappa S, Koci E, Svarcova S, Bezdicka P, Hradil D. Initial stages of metal soaps formation in model paints : the role of humidity. Microchem J. 2020;156:10
85. Beltran, V., Marchetti, A., Nuyts, G., Leeuwestein, M., Sandt, C., Borondics, F., & De Wael, K., “Nanoscale Analysis of Historical Paintings by Means of O-PTIR Spectroscopy: The Identification of the Organic Particles in L’ Arlésienne (Portrait of Madame Ginoux) by Van Gogh”, *Angewandte Chemie International Edition*, *60*(42), 2021, p. 22753-22760.
86. Marchetti, A., Beltran, V., Nuyts, G., Borondics, F., De Meyer, S., Van Bos, M., jaroszewicz, J., Otten, E., Debulpaep, M., De Wael, K., “Novel optical photothermal infrared (O-PTIR) spectroscopy for the noninvasive characterization of heritage glass-metal objects”, *Science advances*, *8*(9), 2022, eabl6769.

87. Spring, M., Ricci, C., Peggie, D. A., Kazarian, S. G., “ATR-FTIR imaging for the analysis of organic materials in paint cross sections: case studies on paint samples from the National Gallery”, London. *Analytical and bioanalytical chemistry*, *392*(1), 2008, p. 37-45.
88. Robinet, L., Corbeil, M. C., “The characterization of metal soaps”, *Studies in conservation*, *48*(1), 2003, p. 23-40.
89. Okamoto, H., and Massalski, T.B., “The Au-Sn (Gold-Tin) System”, Bulletin of Alloy Phase Diagrams, Vol. 5, No. 5, 1984, p. 492-503
90. Yamada, T., Miura, K., Kajihara, M., Kurokawa, N., Sakamoto, K., “Kinetics of reactive diffusion between Au and Sn during annealing at solid-state temperatures”, Materials Science and Engineering A., 390, 2005. p. 118-126,
91. Baheti, V., Kashyap, S., Kumar, P., Chattopadhyay, K., Aloke, P., “Solid state diffusion-controlled growth of the phases in the Au-Sn system, Philosophical magazine, 98, 2017, p. 1-17.
92. Berberich, C., “Studien zu Blattgold und Zwischgold. Herstellung, Materialanalytik, Aspekte zur Verarbeitung und Alterung”, Diplomarbeit, Technische Universität München, Lehrstuhl für Restaurierung, Kunsttechnologie und Konservierungswissenschaft, 2024.
93. Berberich, C., Nothdurft, B., Haettich, A., Schäfer, B., Schmauch, J., Pauly, C., and Koch, M., “Studies on gold leaf and part gold - material, analysis and corrosion”, German archaeometry conference, 2025, Dresden.
https://www.researchgate.net/publication/397435332_Studies_on_gold_leaf_and_part_gold_-_material_analysis_and_corrosion

Supplementary Files

This is a list of supplementary files associated with this preprint. Click to download.

- SupplementaryInformation.docx